

vs  $(3 \cos^2 \theta - 1)/r^3$  for all meso-aryl positions for Fe(TPP)(*t*-BuNC)<sub>2</sub>ClO<sub>4</sub> (and methyl substituents) is given in Figure 4. The slope of the best-fit straight line will yield directly the dipolar contribution to all shifts, while the magnitude of the deviation for the individual data points will yield the contact contribution as previously suggested by La Mar.<sup>7</sup> It is clearly observed that (i) the fit of the shifts to the geometric factor is very poor, (ii) the best fit for the points yields a straight line with a slope very close to zero with large deviations of alternating signs (Table II). Thus, here the magnetic anisotropy is negligible.

Hence, the phenyl proton shifts were analyzed in terms of the contact interaction. At the meso position, the contact shifts for the phenyl protons are large and the presence of sign reversal between the proton and the methyl group indicates that a large amount of  $\pi$  spin density is placed on the phenyl carbons. The lowest vacant  $\pi$  molecular orbital ( $4e \pi^*$ ) exhibits large meso-carbon spin density for low-spin ferric porphyrins.<sup>18</sup> Hence, the contact shift data are consistent only with dominant spin transfer involving Fe  $\rightarrow$  porphyrin  $\pi^*$  charge transfer. Such a mechanism would be expected if alkyl isocyanides acted as pure donor ligands. The large increase of the frequency ( $\bar{\nu}(\text{CN}) \approx 80 \text{ cm}^{-1}$ ) indicates

that this is the case and there is no significant electron flow toward the  $\pi$  orbitals of the ligands.<sup>12</sup>

The small contact shift for pyrrole protons favors the interpretation that negligible spin density is placed on the pyrrole carbons and accounts for the observed downfield shifts. It is interesting to note that the mechanism of spin transfer appears here to give rise to a conclusion opposite to that observed for low-spin ferric bis(imidazole) complexes of a series of synthetic porphyrins.<sup>14</sup> In this latter case, the phenyl proton shifts of Fe(TPP)(Im)<sub>2</sub>Cl were found to be wholly dipolar in origin.

It is noteworthy that the proton NMR data of La Mar et al. have already provided evidence that the magnetic anisotropy is decreased and that the  $\pi$ -contact shifts for the meso position are increased in low-spin dicyano ferric complexes of tetraarylporphyrins as the solvent hydrogen-bonding donor strength increases.<sup>7</sup> Our results are consistent with those reported by these authors since complete protonation of cyanide complexes would lead to isocyanide complexes. In conclusion, the orientation of the unpaired spin density in  $S = 1/2$  ferric porphyrin derivatives is strongly influenced by the nature of the axial ligands since exchanging a nitrogen base (imidazole) for isocyanide leads to completely reverse localization.

**Acknowledgment.** We wish to thank Dr. H. Noel for carrying out the magnetic susceptibility studies.

(18) Zerner, M.; Gouterman, M.; Kobayashi, H. *Theor. Chim. Acta* 1966, 6, 363.

Contribution from the Laboratoire de Biophysique de l'Institut de Biologie Physico-Chimique, Unité Associée au CNRS No. 1089, 13, rue Pierre et Marie Curie, 75005 Paris, France, Section de Biologie de l'Institut Curie, Unité INSERM 219, Centre Universitaire, 91405 Orsay Cedex, France, and Service de Biophysique, Département de Biologie du Centre d'Etudes Nucléaires de Saclay, 91191 Gif-sur-Yvette Cedex, France

## Resonance Raman Spectroscopy of Iron(II) Superstructured Porphyrins: Influence of Porphyrin Distortions on CO and O<sub>2</sub> Ligand Dissociation

Alain Desbois,<sup>\*1a</sup> Michel Momenteau,<sup>1b</sup> and Marc Lutz<sup>1c</sup>

Received June 3, 1988

Resonance Raman spectroscopy has been used to probe the effects of a strap strain on the bonding of O<sub>2</sub> and CO of four synthetic Fe(II) [bis(picket)(handle)]tetraphenylporphyrin derivatives complexed with 1-methylimidazole (Fe<sup>II</sup>[(Piv)<sub>2</sub>C<sub>*n*</sub>](1MeIm)). The strain is introduced by varying the length of the amide-linked handle from 12 to 8 carbon atoms ( $n = 12, 10, 9, 8$ ). In the deoxygenated state, minor structural alterations are characterized for the C<sub>8</sub> derivative only at the tetrapyrrole periphery, the phenyl groups, and the Fe-N(axial ligand) bond. Upon CO binding, a gradual increase of the  $\nu(\text{Fe-CO})$  stretching frequency is found upon handle shortening. The frequency shifts of these modes ( $4\text{--}5 \text{ cm}^{-1}$ ) upon <sup>12</sup>CO  $\rightarrow$  <sup>13</sup>CO isotope substitution are indicative of a linear Fe-CO grouping, confirming recent X-ray crystallographic data on the C<sub>12</sub> and C<sub>8</sub> (Ricard, L.; Weiss, R.; Momenteau, M. *J. Chem. Soc., Chem. Commun.* 1986, 818-820. Fisher, J.; Weiss, R.; Momenteau, M. Unpublished results). The increased frequency of the  $\nu(\text{Fe-CO})$  mode is interpreted in terms of a shortening of the Fe-CO bond in a linear Fe-CO unit perpendicular to the heme plane when the handle length decreases. Upon O<sub>2</sub> binding, the  $\nu(\text{Fe-O}_2)$  stretching mode is found nearly insensitive to the handle length ( $560\text{--}563 \text{ cm}^{-1}$ ). This is the first report for such a low frequency for this mode generally observed in the  $568\text{--}573 \text{ cm}^{-1}$  range for other oxygenated ferroporphyrins and oxyhemoproteins. This frequency lowering is interpreted as corresponding to a deformation of the Fe-O-O angle promoted by an intramolecular H bonding between the bound O<sub>2</sub> and one of the amino groups of the handle. The high-frequency regions of RR spectra of deoxy derivatives show that the core size of five-coordinated complexes is unaffected by the handle shortening. On the other hand, both oxygenated and carbonylated complexes exhibit a gradual frequency increase of the mode  $\nu_4$  accompanied by a gradual frequency decrease of the mode  $\nu_2$  when the handle is shortened. This effect is attributed to increased deformations of the tetrapyrrole skeleton. Comparisons of the O<sub>2</sub>-off rate constants of the four oxygenated complexes with their Fe-ligand bond strengths and porphyrin deformations indicate that porphyrin deformations play a major role in ligand dissociation. Similarly, in the carbon monoxide derivatives, a cancelling effect of the strengthening of the Fe-CO bond by increased porphyrin deformations should explain the near-invariability of the observed CO dissociation rates.

### Introduction

The control of affinities for O<sub>2</sub> and CO in hemoproteins may be regulated by both steric and local polar effects provided by distal amino acid residues.<sup>2</sup> Indeed, CO binds to the iron atom

of simple Fe(II) porphyrins in a linear structure along the heme normal.<sup>3</sup> In hemoglobins and myoglobins, the steric effects of amino acid side chains constituting the distal side of the heme pocket can modify the linear Fe-CO grouping into a tilted and/or bent conformation.<sup>4</sup> Recently, Kuriyan et al.<sup>5</sup> found two clear

(1) (a) Institut de Biologie Physico-Chimique. (b) Institut Curie. (c) Centre d'Etudes Nucléaires.

(2) (a) Perutz, M. F. *Br. Med. Bull.* 1976, 32, 195-208. (b) Caughey, W. S. *Ann. N.Y. Acad. Sci.* 1970, 174, 148-153. (c) Collman, J. P.; Brauman, J. I.; Doxsee, K. M. *Proc. Natl. Acad. Sci. U.S.A.* 1979, 76, 6035-6039.

(3) (a) Hoard, J. L. In *Porphyrins and Metalloporphyrins*; Smith, K. M., Ed.; Elsevier: New York, 1975; pp 317-380. (b) Peng, S. M.; Ibers, J. A. *J. Am. Chem. Soc.* 1976, 98, 8032-8036. (c) Scheidt, W. R.; Haller, K. J.; Fons, M.; Mashiko, T.; Reed, C. A. *Biochemistry* 1981, 20, 3653-3657.

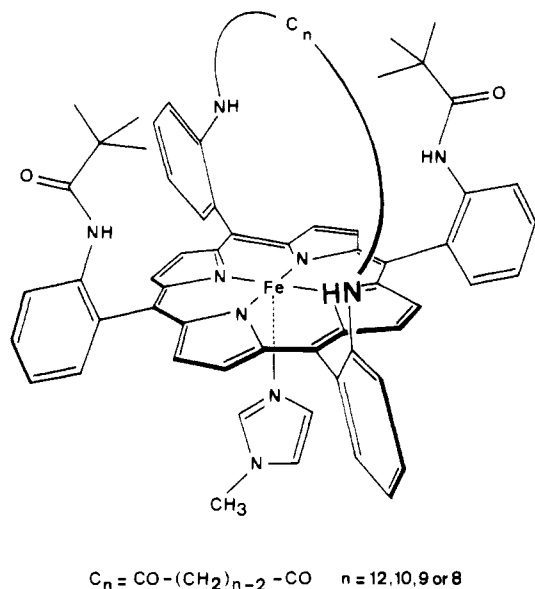


**Figure 1.** Chemical structure of Fe(II) bis(picket)(handle)tetraphenylporphyrins ( $\text{Fe}^{\text{II}}[(\text{Piv})_2\text{C}_n]$ ) complexed with a molecule of 1-methylimidazole.

bent ligand conformations in the crystal structure of Fe(II)-myoglobin-CO at a resolution of 1.5 Å. In comparison to a linear structure, these distortions are obviously expected to cause changes in the intrinsic ligand affinity. On the other hand,  $\text{O}_2$  binds both simple Fe(II) porphyrins and hemoproteins in an end-on bent structure.<sup>6</sup> However, H bonding between the bound  $\text{O}_2$  and a proton of a distal histidyl imidazole residue may stabilize the ligand binding of oxyhemoglobin and oxymyoglobin.<sup>6d,7</sup> Therefore, the hemoproteins may discriminate binding of  $\text{O}_2$  from that of the CO ligand.<sup>8</sup> This differentiation is believed to be a detoxification mechanism for CO-complexed hemoproteins.<sup>2c</sup>

Numerous model compounds that reversibly bind these gaseous ligands have been prepared in order to determine the main factors governing the ligand binding in the native hemoproteins.<sup>9</sup> In order to study the influence of the distal steric effect in the discrimination between CO and  $\text{O}_2$  ligations, a new series of single-face-hindered Fe(II) tetraphenylporphyrin compounds was recently synthesized and characterized.<sup>10</sup> These compounds are "hybrid" models, being intermediate between the "picket-fence" Fe(II) porphyrin<sup>9a</sup> and the "basket-handle" Fe(II) porphyrins.<sup>9d</sup> They indeed have two pivalamido "pickets" and one polymethylene "handle" of variable length in a cross configuration<sup>9d,10</sup> (Figure 1). The variable "handle" allows us to change the ligand cavity size while the two

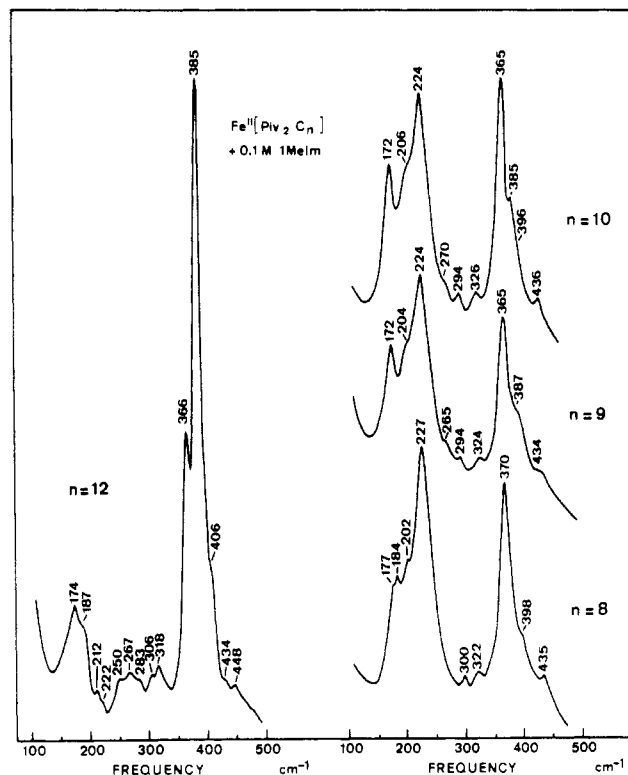


**Figure 2.** Low-frequency regions (100–500  $\text{cm}^{-1}$ ) of resonance Raman spectra of  $\text{Fe}^{\text{II}}[(\text{Piv})_2\text{C}_n]$  in benzene containing 0.1 M 1-methylimidazole. Experimental conditions: heme concentration 1 mM; excitation wavelength 441.6 nm; summation of four scans.

pickets hold the "handle" in a central position. Affinity and kinetic data for CO and  $\text{O}_2$  on the iron(II) derivative of these bis(picket)(handle)iron(II) tetraphenylporphyrins ( $\text{Fe}^{\text{II}}[(\text{Piv})_2\text{C}_n]$ )<sup>11</sup> were measured in the presence of 1-methylimidazole (1MeIm), which preferentially binds to the unhindered side of porphyrins<sup>9d,10</sup> (Figure 1). The most striking effect is that the equilibrium binding constant for CO can be decreased by a factor of 2500 while the  $\text{O}_2$  constant changes by less than a factor of 3.5 upon decreasing the "handle" length by four methylene units ( $\text{C}_{12} \rightarrow \text{C}_8$ ).<sup>9d</sup>

An understanding of the structural origins of the trends in ligand binding of these heme models is certainly of importance in the assessment of structure–function relationship in hemoproteins. For this purpose, we have examined the resonance Raman (RR) spectra of deoxygenated, carbonylated, and oxygenated derivatives of  $\text{Fe}^{\text{II}}[(\text{Piv})_2\text{C}_n](1\text{MeIm})$ . Since RR spectroscopy is able to monitor the vibrational modes of porphyrin bonds and of metal–axial ligand bonds,<sup>12</sup> the observed spectral differences are interpreted in terms of electronic, environmental, and structural parameters that can influence the ligand association–dissociation.

### Experimental Section

**Ferrous Porphyrins.** The Fe(III)-bis(picket)(handle)porphyrin-chloride complexes used in this work were synthesized and characterized by methods previously described.<sup>10</sup> The sample solution (2 mL, 0.2–1 mM heme and 100 mM 1-methylimidazole) was placed in a rubber-sealed glass cell. The solution was deoxygenated by flushing with pure argon gas and, then, reduced by using a classic two-phase system.<sup>10</sup>  $\text{O}_2$  or CO was introduced at a pressure of 1 atm.  $^{18}\text{O}_2$  and  $^{13}\text{CO}$  gas with isotope enrichment of 98% and 99%, respectively (Bureau des isotopes stables, Centre d'Etudes Nucléaires de Saclay), were used for the isotopic experiments.

- (4) (a) Huber, R.; Epp, O.; Formanek, H. *J. Mol. Biol.* **1970**, *52*, 349–354. (b) Norwell, J. C.; Nunes, A. C.; Schoenborn, B. P. *Science* **1975**, *190*, 568–570. (c) Padian, E. A.; Love, W. E. *J. Biol. Chem.* **1975**, *249*, 4067–4078. (d) Heidner, E. J.; Ladner, R. C.; Perutz, M. F. *J. Mol. Biol.* **1976**, *104*, 707–722. (e) Steigemann, W.; Weber, E. *J. Mol. Biol.* **1979**, *127*, 309–338. (f) Baldwin, J. M. *J. Mol. Biol.* **1980**, *136*, 103–128.
- (5) Kuriyan, J.; Wilz, S.; Karplus, M.; Petsko, G. A. *J. Mol. Biol.* **1986**, *192*, 133–154.
- (6) (a) Collman, J. P.; Gagne, R. R.; Reed, C. A.; Robinson, W. T.; Rodley, G. A. *Proc. Natl. Acad. Sci. U.S.A.* **1974**, *71*, 1326–1329. (b) Phillips, S. E. V. *J. Mol. Biol.* **1980**, *142*, 531–554. (c) Jameson, G. B.; Molinaro, F. S.; Ibers, J. A.; Collman, J. P.; Brauman, J. I.; Rose, E.; Suslick, K. S. *J. Am. Chem. Soc.* **1980**, *102*, 3224–3237. (d) Shaanan, B. *J. Mol. Biol.* **1983**, *171*, 31–59.
- (7) Phillips, S. E. V.; Schoenborn, B. P. *Nature (London)* **1981**, *292*, 81–82.
- (8) Antonini, E.; Brunori, M. In *Hemoglobin and Myoglobin in Their Reactions with Ligand*; Neuberger, A., Tatum, E. L., Eds.; North-Holland: Amsterdam, 1971; pp 55–97.
- (9) (a) Collman, J. P.; Halbert, T. R.; Suslick, K. S. In *Metal Ion Activation of Dioxygen*; Spiro, T. G., Ed.; Wiley-Interscience: New York, 1980; pp 1–72. (b) Traylor, T. G.; Traylor, P. S. *Annu. Rev. Biophys. Bioeng.* **1982**, *11*, 105–127. (c) Jameson, G. B.; Ibers, J. A. *Comments Inorg. Chem.* **1983**, *2*, 97–126. (d) Momenteau, M. *Pure Appl. Chem.* **1986**, *58*, 1493–1502.
- (10) Momenteau, M.; Loock, B.; Tetreau, C.; Lavalette, D.; Croisy, A.; Schaeffer, C.; Huel, C.; Lhoste, J. M. *J. Chem. Soc., Perkin Trans. 2* **1987**, 249–257.

- (11) Abbreviations used: TPP = 5,10,15,20-tetraphenylporphyrin; (Piv)<sub>4</sub> = picket-fence porphyrin; (Piv)<sub>2</sub>C<sub>n</sub> = α,α-5,15-[2,2'-(X)diphenyl]-α,α-10,20-bis(o-pivalamidophenyl)porphyrin (n = 12, X = dodecanediamido; n = 10, X = decanediamido; n = 9, X = nonanediamido; and n = 8, X = octanediamido); 1MeIm = 1-methylimidazole; RR = resonance Raman; IR = infrared. In Table I, a and e stand for amide-linked and ether-linked chains of basket-handle porphyrins.
- (12) (a) Spiro, T. G. *Adv. Protein Chem.* **1985**, *37*, 111–159. (b) Yu, N.-T. *Methods Enzymol.* **1986**, *130*, 350–409. (c) Kitagawa, T.; Ozaki, Y. In *Struct. Bonding* **1987**, *64*, 71–114.

**Resonance Raman Spectroscopy.** The apparatus and techniques have been described previously.<sup>13</sup> The 441.6-nm emission of a He-Cd laser (Liconix Model 4050) was used.

An improvement in signal to noise ratio of RR spectra was achieved by summation of 4–10 scans of 200, 400, or 600  $\text{cm}^{-1}$  in the low- or high-frequency region using a multichannel analyzer (Tracor Northern TN 1710). Under these conditions, the absolute frequencies of the RR bands were determined within a 1–3- $\text{cm}^{-1}$  uncertainty, depending on their intensities, while frequency shifts had been determined within 1–2  $\text{cm}^{-1}$ .

In order to minimize the ligand photodissociation that may occur during laser illumination, three conditions were observed: (i) the solution was stirred, (ii) low laser powers ( $\leq 5$  mW) were used, and (iii) the laser beam was defocused. Under these conditions, no detectable photodissociation was observed in the RR spectra of carbonylated and oxygenated complexes.

## Results and Discussion

**Deoxygenated Complexes.** Figure 2 shows the low-frequency regions (100–500  $\text{cm}^{-1}$ ) of RR spectra of the  $\text{Fe}^{\text{II}}[(\text{Piv})_2\text{C}_n]$  compounds ( $n = 12, 10, 9, 8$ ) in benzene containing 0.1 M 1MeIm. Systematic studies on iron(II) tetraphenylporphyrin ( $\text{Fe}^{\text{II}}\text{TPP}$ ) derivatives showed that the observation of a strong band at 380–390  $\text{cm}^{-1}$  is characteristic of a low-spin six-coordinated complex.<sup>14</sup>

From the normal-coordinate analysis of nickel(II) octaethylporphyrin,<sup>15</sup> Stein and co-workers<sup>16</sup> assigned this band to a deformation mode of the porphyrin macrocycle ( $\nu_8$ ). On the other hand, the observation of a medium band in the 365–370- $\text{cm}^{-1}$  region of RR spectra of  $\text{Fe}^{\text{II}}\text{TPP}$  derivatives is indicative of high-spin five-coordination.<sup>14</sup>

The spectra shown in Figure 2 indicate that the compound containing the longest handle ( $n = 12$ ) is essentially six-coordinated ( $\nu_8$  at 385  $\text{cm}^{-1}$ ). However, the presence of a band of 366  $\text{cm}^{-1}$  reveals the simultaneous existence of a five-coordinated form even at 0.1 M 1MeIm. For the porphyrins with a 10- or 9-carbon-containing handle, the complexes are predominantly five-coordinated, taking into account the relative intensity of the ca. 365- and 386- $\text{cm}^{-1}$  bands (Figure 2). Finally, the lack of any band at  $\sim 386$   $\text{cm}^{-1}$  in the spectrum of  $\text{Fe}^{\text{II}}[(\text{Piv})_2\text{C}_8]$  indicates that the six-coordinated complex is absent under these conditions (Figure 2). These qualitative estimations on the coordination state of  $\text{Fe}^{\text{II}}[(\text{Piv})_2\text{C}_n]$  porphyrins with 1MeIm are in agreement with previous equilibrium measurements.<sup>10</sup>

We note that  $\nu_8$  is increased from 365–366  $\text{cm}^{-1}$  in the spectra of  $\text{Fe}^{\text{II}}[(\text{Piv})_2\text{C}_n](1\text{MeIm})$  (with  $n = 12, 10, 9$ ) to 370  $\text{cm}^{-1}$  in the spectrum of  $\text{Fe}^{\text{II}}[(\text{Piv})_2\text{C}_8](1\text{MeIm})$  (Figure 2). This frequency shift indicates that the shortest "handle" induces some slight porphyrin distortions.

The 1MeIm complex of the "picket-fence" Fe(II) porphyrin ( $\text{Fe}^{\text{II}}[(\text{Piv})_4](1\text{MeIm})$ ) exhibits a band at 225  $\text{cm}^{-1}$ , which was assigned to the stretching mode of the  $\text{Fe}^{\text{II}}\text{-N}(1\text{MeIm})$  bond.<sup>17a</sup> The presence of a strong band at 224  $\text{cm}^{-1}$  in the spectra of  $\text{Fe}^{\text{II}}[(\text{Piv})_2\text{C}_n](1\text{MeIm})$  ( $n = 10, 9$ ) indicates that the Fe-N(1MeIm) bond strength does not significantly differ in these two complexes and in  $\text{Fe}^{\text{II}}[(\text{Piv})_4](1\text{MeIm})$ . The slight increase in frequency of the corresponding band of  $\text{Fe}^{\text{II}}[(\text{Piv})_2\text{C}_8](1\text{MeIm})$  (227  $\text{cm}^{-1}$ ) may reflect a slight strengthening of the axial bond.

Stein et al.<sup>16</sup> assigned a band observed at 197  $\text{cm}^{-1}$  in the RR spectra of metal-free TPP to a pure phenyl-porphyrin stretching mode. This frequency appears too low for such a mode. Indeed, a normal-coordinate treatment on biphenyl assigned the totally

symmetric stretching mode of the inter-ring bond at 1003  $\text{cm}^{-1}$ .<sup>18</sup> Two other  $A_{1g}$  modes involving the phenyl-phenyl stretching were calculated at 1285 and 315  $\text{cm}^{-1}$  but were coupled with in-plane deformations of phenyl groups. Therefore, the assignment of the  $C_m$ -phenyl stretching modes to a band at 1230–1240  $\text{cm}^{-1}$  in the RR spectra of  $\text{Fe}^{\text{II}}$ - and  $\text{Fe}^{\text{III}}\text{TPP}$  derivatives appears the most likely.<sup>14a</sup>

On the other hand, at Soret resonance, various  $\text{Fe}^{\text{II}}$ - and  $\text{Fe}^{\text{III}}$ -TPP complexes exhibit a polarized Raman band at 195–205  $\text{cm}^{-1}$ .<sup>19</sup> A systematic study on the RR spectra of complexes of Fe(II) and Fe(III) "basket-handle" porphyrins<sup>9d</sup> in which the phenyl groups are substituted in one ortho position shows this band at a lower frequency (166–190  $\text{cm}^{-1}$ ).<sup>19b</sup> This mass effect as well as the previously cited normal-coordinate treatment on biphenyl<sup>18</sup> allows us to propose that the 166–205- $\text{cm}^{-1}$  band of  $\text{Fe}^{\text{II}}$ - and  $\text{Fe}^{\text{III}}\text{TPP}$  derivatives corresponds to a stretching mode of the  $C_m$ -phenyl bonds involving strong contributions from both porphyrins and phenyl deformations. On the other hand, the frequency of the 166–205- $\text{cm}^{-1}$  band is sensitive to the spin state or to the coordination number of the iron atom, the high-spin pentacoordinated complexes exhibiting lower frequencies than the low-spin hexacoordinated one.<sup>19b</sup> The RR spectrum of  $\text{Fe}^{\text{II}}[(\text{Piv})_2\text{C}_{12}]$  in the presence of 1-MeIm illustrates this trend as well. The bands observed at 174 and 187  $\text{cm}^{-1}$  are indeed attributed to the mono and bis 1MeIm forms, respectively (Figure 2). Furthermore, the frequency of this band may be used as an indicator of "handle" tension. Indeed,  $\text{Fe}^{\text{II}}[(\text{Piv})_2\text{C}_n](1\text{MeIm})$  complexes (with  $n = 12, 10, 9$ ) exhibit the corresponding band at 172–174  $\text{cm}^{-1}$  (Figure 2), in accordance with the RR data on pentacoordinated "basket-handle" iron porphyrins.<sup>19b</sup> In the spectra of  $\text{Fe}^{\text{II}}[(\text{Piv})_2\text{C}_8](1\text{MeIm})$ , the corresponding band is split and the components are shifted to higher frequencies (177 and 184  $\text{cm}^{-1}$ ). These spectral modifications indicate that the shortest handle promotes inequivalent contractions and/or distortions at the  $C_m$ -phenyl bonds.

The high-frequency regions of RR spectra of metallo TPP derivatives exhibit two strong bands at 1340–1370 and 1540–1570  $\text{cm}^{-1}$  when observed under pre-Soret resonance conditions.<sup>19</sup> The frequencies of these bands are known to be sensitive to changes in the oxidation and/or spin state of the metal atom.<sup>14</sup>

The polarized band at 1340–1370  $\text{cm}^{-1}$  is assigned to  $\nu_4$  and corresponds to a  $\nu(C_a\text{-N}(\text{pyrrole}))$  stretching mode coupled with a deformation of  $C_a\text{-C}_m$  bonds.<sup>15,16</sup> Its frequency is known to depend upon the electron density at the  $\pi^*(e_g)$  orbital of the porphyrin core.<sup>12</sup> Five-coordinated high-spin complexes of  $\text{Fe}^{\text{II}}\text{TPP}$  and of Fe(II) "basket-handle" porphyrins exhibit  $\nu_4$  at 1342–1345  $\text{cm}^{-1}$  while their six-coordinated low-spin ferrous complexes have  $\nu_4$  in the 1353–1370- $\text{cm}^{-1}$  range, depending on the nature of axial ligands.<sup>14b,c,19b</sup>

The polarized band at 1537–1570  $\text{cm}^{-1}$  ( $\nu_2$ ) is spin-state sensitive. It is observed at 1537–1542 and 1553–1566  $\text{cm}^{-1}$  for high-spin and low-spin complexes of  $\text{Fe}^{\text{II}}\text{TPP}$  and of Fe(II) "basket-handle" porphyrins, respectively.<sup>14,19b</sup> In spite of its assignment to a  $\nu(C_b\text{-C}_b)$  stretching mode,<sup>15,16</sup> the frequency of  $\nu_2$  has been reliably correlated with the porphyrin center (Ct) to N(pyrrole) distance.<sup>20</sup>

As observed in the low-frequency regions, the deoxygenated form of  $\text{Fe}^{\text{II}}[(\text{Piv})_2\text{C}_{12}]$  with 0.1 M 1MeIm exhibits a RR spectrum essentially corresponding to a bis(base) complex since  $\nu_4$  and  $\nu_2$  are observed at 1356 and 1555  $\text{cm}^{-1}$ , respectively (Figures 3 and 4). For the other  $\text{Fe}^{\text{II}}[(\text{Piv})_2\text{C}_n]$  complexes ( $n = 10, 9, 8$ ),  $\nu_4$  and  $\nu_2$  are characteristic of five-coordinated forms (1345 and 1541

(13) (a) Desbois, A.; Lutz, M.; Banerjee, R. *Biochemistry* **1979**, *18*, 1510–1518. (b) Desbois, A.; Henry, Y.; Lutz, M. *Biochim. Biophys. Acta* **1984**, *785*, 148–160.

(14) (a) Burke, J. M.; Kincaid, J. R.; Spiro, T. G. *J. Am. Chem. Soc.* **1978**, *100*, 6077–6083. (b) Burke, J. M.; Kincaid, J. R.; Peters, S.; Gagne, R. R.; Collman, J. P.; Spiro, T. G. *J. Am. Chem. Soc.* **1978**, *100*, 6083–6088. (c) Oshio, H.; Ama, T.; Watanabe, T.; Kincaid, J.; Nakamoto, K. *Spectrochim. Acta* **1984**, *40A*, 863–870. (d) Proniewicz, L. M.; Bajdor, K.; Nakamoto, K. *J. Phys. Chem.* **1986**, *90*, 1760–1766.

(15) Abe, M.; Kitagawa, T.; Kyogoku, Y. *J. Chem. Phys.* **1978**, *69*, 4526–4534.

(16) Stein, P.; Ulman, A.; Spiro, T. G. *J. Phys. Chem.* **1984**, *88*, 369–374.

(17) (a) Hori, H.; Kitagawa, T. *J. Am. Chem. Soc.* **1980**, *102*, 3608–3613. (b) Desbois, A.; Lutz, M. Unpublished data.

(18) Zerbi, G.; Sandroni, S. *Spectrochim. Acta* **1968**, *24A*, 511–528.

(19) (a) Schick, G. A.; Bocian, D. F. *J. Am. Chem. Soc.* **1983**, *105*, 1830–1838. (b) Desbois, A.; Momenteau, M.; Lutz, M. Unpublished spectra.

(20) (a) Spaulding, D. L.; Chang, C. C.; Yu, N.-T.; Felton, R. H. *J. Am. Chem. Soc.* **1975**, *97*, 2517–2525. (b) Huang, P. V.; Pommier, J.-C. *C. R. Seances Acad. Sci., Ser. C* **1977**, *285*, 519–522. (c) Spiro, T. G.; Stong, J. D.; Stein, P. *J. Am. Chem. Soc.* **1979**, *101*, 2648–2655. (d) Stong, J. D.; Spiro, T. G.; Kubaska, R. J.; Shupack, S. I. *J. Raman Spectrosc.* **1980**, *9*, 312–314. (e) Parthasarathi, N.; Hansen, C.; Yamaguchi, S.; Spiro, T. G. *J. Am. Chem. Soc.* **1987**, *109*, 3865–3871.

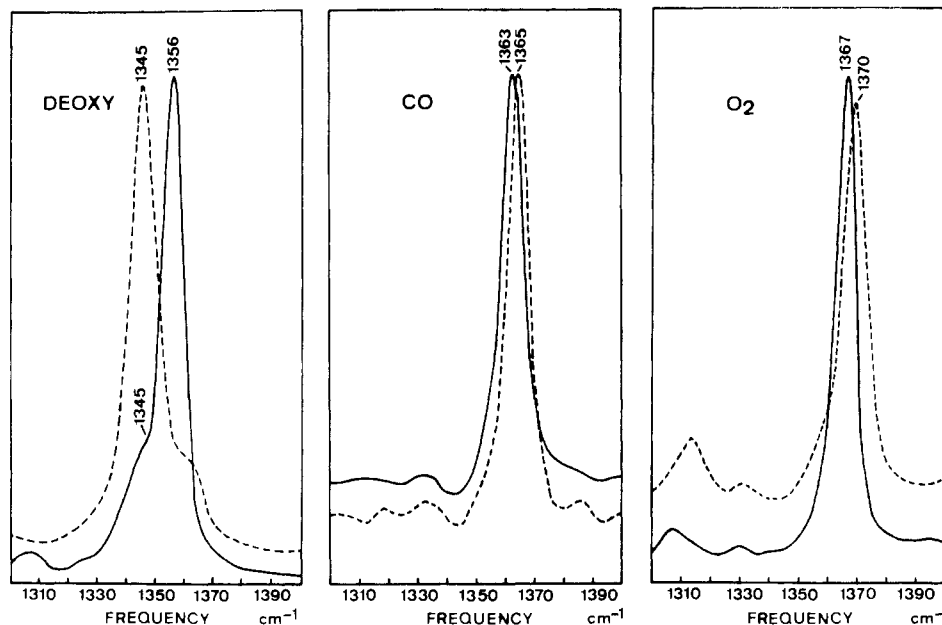


Figure 3. Resonance Raman spectra in the 1300–1400-cm<sup>-1</sup> region of deoxy, CO, and O<sub>2</sub> forms of Fe<sup>II</sup>[(Piv)<sub>2</sub>C<sub>12</sub>](1MeIm) (solid lines) and of Fe<sup>II</sup>[(Piv)<sub>2</sub>C<sub>8</sub>](1MeIm) (dotted lines) (summation of four scans).

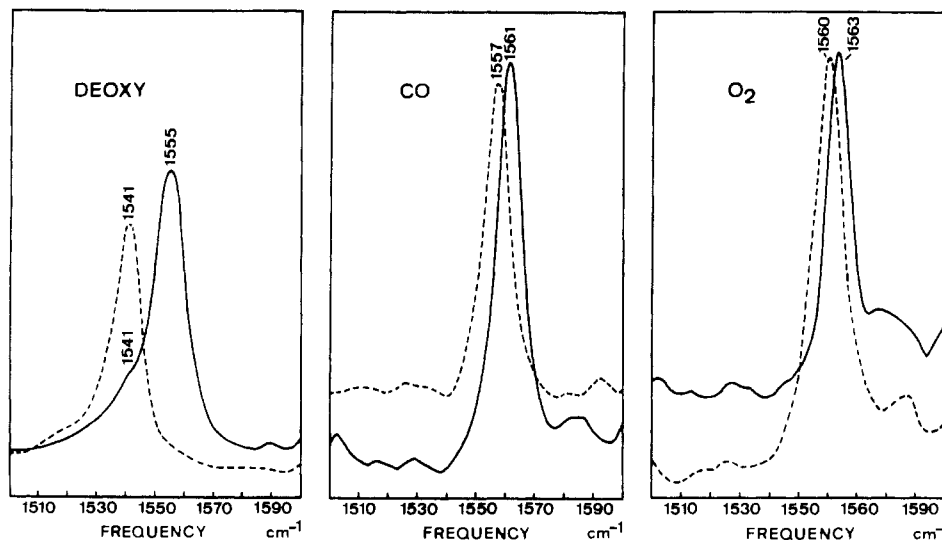


Figure 4. Resonance Raman spectra in the 1500–1600-cm<sup>-1</sup> region of deoxy, CO, and O<sub>2</sub> forms of Fe<sup>II</sup>[(Piv)<sub>2</sub>C<sub>12</sub>](1MeIm) (solid lines) and of Fe<sup>II</sup>[(Piv)<sub>2</sub>C<sub>8</sub>](1MeIm) (dotted lines) (summation of four scans).

cm<sup>-1</sup>, respectively) (Figures 3 and 4 for the C<sub>8</sub> derivative). Therefore, the handle shortening has no influence on the high-frequency modes of the five-coordinated complexes.

The frequency of  $\nu_2$  (in cm<sup>-1</sup>) is correlated with the Ct–N–pyrrole) distance  $d$  (in Å) by the relation

$$\nu_2 = K(A - d) \quad (1)$$

where  $K$  and  $A$  are constants.<sup>20</sup> However, large deviations from linearity have been observed for some metalloporphyrin complexes and have been associated with porphyrin deformations (doming or ruffling).<sup>20</sup> In Figure 5, we have plotted the frequency of  $\nu_2$  versus the Ct–N distance for various metallo TPP derivatives. The experimental points permit us to determine two couples of limiting values for  $A$  and  $K$ . Line I is associated with the majority of hexacoordinated complexes and is characterized by  $K$  and  $A$  values of 248.4 cm<sup>-1</sup> Å<sup>-1</sup> and 8.29 Å, respectively. A second group of aligned points corresponds to the majority of pentacoordinated complexes (line II) with  $K$  and  $A$  values of 372.5 cm<sup>-1</sup> Å<sup>-1</sup> and 6.17 Å, respectively (Figure 5). Taking these latter values for the calculation of the core size of Fe<sup>II</sup>[(Piv)<sub>2</sub>C<sub>*n*</sub>](1MeIm) ( $\nu_2 = 1541$  cm<sup>-1</sup>), we obtain  $d = 2.033$  Å, in agreement with the crystal structure of Fe<sup>II</sup>[(Piv)<sub>2</sub>C<sub>8</sub>](1MeIm), which gives Ct–N = 2.051 ± 0.021 Å.<sup>21</sup>

**Carbon Monoxide Adducts.** The Fe–CO stretching and bending vibrations of carbonylated complexes of hemoproteins and model compounds have been detected in the 450–600-cm<sup>-1</sup> regions of RR spectra.<sup>24</sup> The corresponding regions of RR spectra

- (21) Momenteau, M.; Scheidt, W. R.; Eigenbrot, C. W.; Reed, C. A. *J. Am. Chem. Soc.* **1988**, *110*, 1207–1215.
- (22) (a) Chottard, G.; Battioni, P.; Battioni, J.-P.; Lange, M.; Mansuy, D. *Inorg. Chem.* **1981**, *20*, 1718–1722. (b) Chottard, G.; Schappacher, M.; Ricard, L.; Weiss, R. *Inorg. Chem.* **1984**, *23*, 4557–4561. (c) Crisanti, M. A.; Spiro, T. G.; English, D. R.; Hendrickson, D. N.; Suslick, K. S. *Inorg. Chem.* **1984**, *23*, 3897–3901.
- (23) (a) Scheidt, W. R.; Gouterman, M. In *Iron Porphyrins*; Part I: Lever, A. B. P., Gray, H. B., Eds.; Addison-Wesley: Reading, MA, 1983; pp 89–139. (b) Goedken, V. L.; Deakin, M. R.; Bottomley, L. A. *J. Chem. Soc., Chem. Commun.* **1982**, 607–608.
- (24) (a) Tsubaki, M.; Srivastava, R. B.; Yu, N.-T. *Biochemistry* **1982**, *21*, 1132–1140. (b) Armstrong, R. S.; Irwin, M. J.; Wright, P. E. *J. Am. Chem. Soc.* **1982**, *104*, 626–627. (c) Kerr, E. A.; Mackin, H. C.; Yu, N.-T. *Biochemistry* **1983**, *22*, 4373–4379. (d) Yu, N.-T.; Kerr, E. A.; Ward, B.; Chang, C. K. *Biochemistry* **1983**, *22*, 4534–4540. (e) Yu, N.-T.; Benko, B.; Kerr, E. A.; Gersonde, K. *Proc. Natl. Acad. Sci. U.S.A.* **1984**, *81*, 5106–5110. (f) Carson, S. D.; Constantinidis, I.; Satterlee, J. D.; Ondrias, M. R. *J. Biol. Chem.* **1985**, *260*, 8741–8745. (g) Kerr, E. A.; Yu, N.-T.; Bartnicki, D. E.; Mizukami, H. *J. Biol. Chem.* **1985**, *260*, 8360–8365.

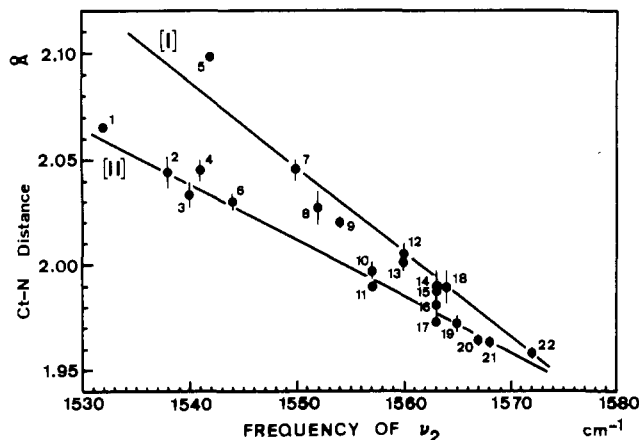


**Figure 5.** Core size (Å) versus frequency of the  $\nu_2$  mode ( $\text{cm}^{-1}$ ) of various metallotetraphenylporphyrin derivatives: (1)  $\text{Mn}^{\text{II}}\text{TPP}(2\text{MeImH})$ ; (2)  $\text{Fe}^{\text{II}}\text{TPP}(2\text{MeImH})$ ; (3)  $\text{Fe}^{\text{II}}[(\text{Piv})_4](2\text{MeImH})$ ; (4)  $\text{Fe}^{\text{III}}\text{TPP}(\text{DMSO})_2$ ; (5)  $\text{Sn}^{\text{IV}}\text{TPP}(\text{Cl})_2$ ; (6)  $\text{Fe}^{\text{II}}\text{TPP}(\text{SC}_2\text{H}_5)_2$ ; (7)  $\text{Fe}^{\text{III}}\text{TPP}(\text{DMSO})_2$ ; (8)  $[\text{Fe}^{\text{III}}\text{TPP}]_2\text{O}$ ; (9)  $\text{Fe}^{\text{III}}\text{TPP}(\text{Cl})$ ; (10)  $\text{Fe}^{\text{II}}\text{TPP}(1\text{MeIm})_2$ ; (11)  $\text{Mn}^{\text{III}}\text{TPP}(\text{Cl})$ ; (12)  $\text{Fe}^{\text{III}}\text{TPP}(\text{Pip})_2$ ; (13)  $\text{Cu}^{\text{II}}\text{TPP}$ ; (14)  $\text{Fe}^{\text{III}}\text{TPP}(\text{ImH})_2$ ; (15)  $\text{Fe}^{\text{II}}\text{TPP}(\text{CS})(\text{py})$ ; (16)  $\text{Fe}^{\text{II}}[(\text{Piv})_4](1\text{MeIm})(\text{O}_2)$ ; (17)  $\text{Co}^{\text{II}}\text{TPP}(2\text{MeImH})$ ; (18)  $\text{Fe}^{\text{III}}\text{TPP}(1\text{MeIm})_2$ ; (19)  $\text{Fe}^{\text{II}}\text{TPP}$ ; (20)  $[\text{Fe}^{\text{III}}\text{TPP}]_2\text{N}$ ; (21)  $[\text{Fe}^{\text{III}}\text{TPP}]_2\text{C}$ ; (22)  $\text{Ni}^{\text{II}}\text{TPP}$ . The RR data are from ref 14, 17a, 19, 20, and 22. The crystallographic data are from ref 23.

of  $^{12}\text{CO}$  and  $^{13}\text{CO}$  complexes of  $\text{Fe}^{\text{II}}[(\text{Piv})_2\text{C}_n](1\text{MeIm})$  are displayed in Figure 6. Figure 6A clearly shows a  $4\text{-cm}^{-1}$  downshift of a  $488\text{-cm}^{-1}$  band upon isotope substitution in  $\text{Fe}^{\text{II}}[(\text{Piv})_2\text{C}_{12}](1\text{MeIm})(\text{CO})$ , as also observed for the Fe—CO stretching mode of  $\text{Fe}^{\text{II}}[(\text{Piv})_4](1\text{MeIm})(\text{CO})$  at  $489\text{ cm}^{-1}$ .<sup>24c</sup> Thus, in comparison to the picket-fence complex, the substitution of two pickets by a handle containing 12 carbon atoms does not significantly influence the Fe—CO bond structure. When the handle length is decreased from 12 to 10 and 9 carbon atoms, a gradual increase in the frequency of the isotope-sensitive line is observed, from 488 to 497 and  $506\text{ cm}^{-1}$ , respectively (Figure 6B,C). We assign these bands, which are downshifted by 3 and  $5\text{ cm}^{-1}$  upon  $^{12}\text{CO} \rightarrow ^{13}\text{CO}$  substitution, to the Fe—CO stretching mode.

The RR spectrum of  $\text{Fe}^{\text{II}}[(\text{Piv})_2\text{C}_8](1\text{MeIm})(\text{CO})$  appears more complex than the preceding spectra (Figure 6D). Indeed, three isotope-sensitive bands are observed at 497, 515, and  $576\text{ cm}^{-1}$ . The first two bands are shifted by 4 and  $5\text{ cm}^{-1}$  upon CO substitution, respectively. We hence assign them to  $\nu(\text{Fe—CO})$  stretching modes. This shows that in the case of the shortest handle interacting with the ligand, at least two conformations of the Fe—CO grouping are allowed. On the other hand, the  $576\text{-cm}^{-1}$  band is downshifted by  $21\text{ cm}^{-1}$  (Figure 6D). Deformation modes of the Fe—CO grouping of pyrrole-substituted porphyrins generally have been observed in the  $559\text{--}580\text{-cm}^{-1}$  region.<sup>24</sup> Although the present isotope shift is slightly stronger than those observed ( $11\text{--}19\text{ cm}^{-1}$ )<sup>24</sup> or expected ( $18\text{ cm}^{-1}$ )<sup>24a</sup> for these porphyrins, we tentatively assign the  $576\text{-cm}^{-1}$  band of  $\text{Fe}^{\text{II}}[(\text{Piv})_2\text{C}_8](1\text{MeIm})(\text{CO})$  to a Fe—CO bending mode.

The infrared frequencies of the  $\nu(\text{C=O})$  stretching modes of the present  $\text{Fe}^{\text{II}}[(\text{Piv})_2\text{C}_n](1\text{MeIm})(\text{CO})$  complexes were previously published.<sup>10</sup> They are listed in Table I together with IR and RR data on the  $\nu(\text{Fe—CO})$  and  $\nu(\text{C=O})$  stretching modes of carbonylated complexes of various Fe(II) tetraphenylporphyrin derivatives. The frequency values of the  $\nu(\text{Fe—CO})$  and  $\nu(\text{CO})$  stretching modes cannot directly distinguish a linear Fe—CO geometry from a bent conformation. However, Yu et al.<sup>24d</sup> proposed a relation expected to estimate the Fe—CO bond angle

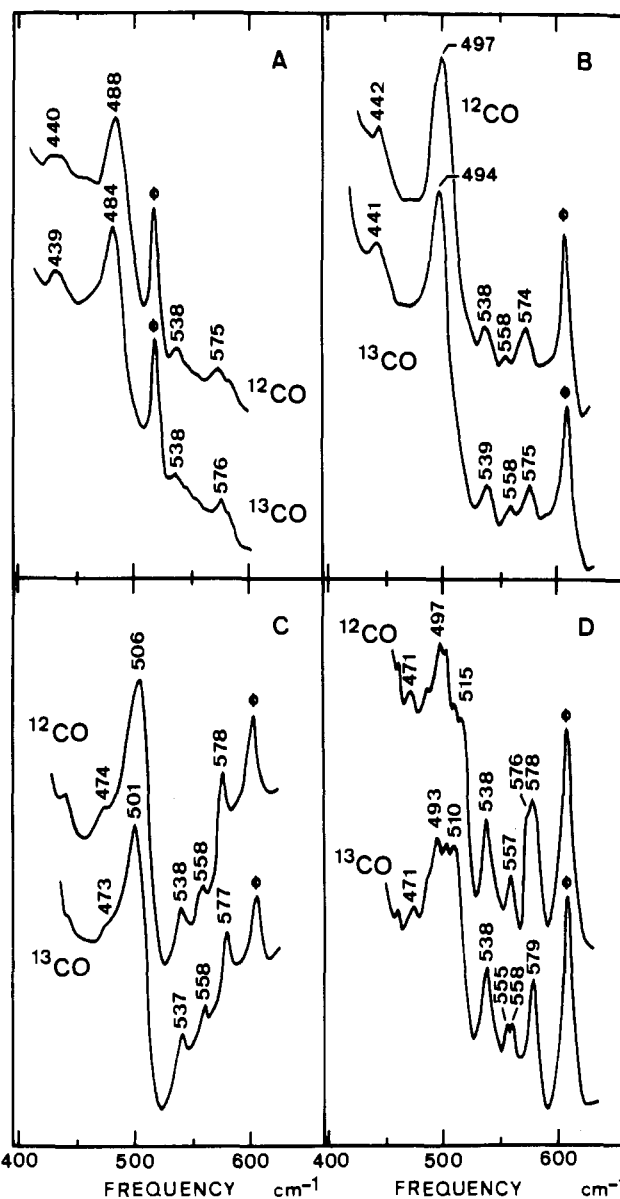


**Figure 6.** CO isotope effect on the low-frequency regions ( $400\text{--}600\text{ cm}^{-1}$ ) of resonance Raman spectra of  $\text{Fe}^{\text{II}}[(\text{Piv})_2\text{C}_n](1\text{MeIm})(\text{CO})$  in benzene or toluene (summation of four to eight scans;  $\phi$  denotes solvent bands): (A)  $n = 12$ ; (B)  $n = 10$ ; (C)  $n = 9$ ; (D)  $n = 8$ .

of CO complexes of "strapped" Fe(II) hemes and of hemoproteins. Unfortunately, Li and Spiro<sup>27a</sup> recently showed that Yu's equation is not valid in the case of the Fe—CO grouping, for which the interaction force constant ( $H$ ) actually cannot be neglected. Using the crystallographic<sup>26a</sup> ( $d_1(\text{Fe—C}) = 1.73\text{ \AA}$ ;  $d_2(\text{C—O}) = 1.15\text{ \AA}$ ;  $\angle\text{Fe—C—O} = 180^\circ$ ) as well as the present vibrational data available for the  $\text{Fe}^{\text{II}}[(\text{Piv})_2\text{C}_{12}](1\text{MeIm})(\text{CO})$  complex (Table I), we have carried out a normal-coordinate calculation on a simple linear triatomic FeCO grouping.<sup>27b,c</sup> Using the set of force constant values  $K_1(\text{Fe—C}) = 2.80\text{ mdyn \AA}^{-1}$ ,  $K_2(\text{C=O}) = 14.5\text{ mdyn \AA}^{-1}$ , and  $H(\text{FeCO}) = 0.22\text{ mdyn \AA}^{-1}$ , we obtained the theoretical frequencies  $\nu(\text{Fe—}^{12}\text{CO}) = 488.4\text{ cm}^{-1}$ ,  $\nu(\text{Fe—}^{13}\text{CO}) = 483.5\text{ cm}^{-1}$ ,  $\nu(^{12}\text{CO}) = 1957.7\text{ cm}^{-1}$ , and  $\nu(^{13}\text{CO}) = 1910.2\text{ cm}^{-1}$ . These values are all in good agreement with the experimental frequencies (488, 484, 1958, and  $1912\text{ cm}^{-1}$ , respectively). This calculation also gives theoretical frequencies for the  $\delta(\text{Fe—}^{12}\text{CO})$  and  $\delta(\text{Fe—}^{13}\text{CO})$  modes at  $580.4$  and  $563.3\text{ cm}^{-1}$ , respectively. Although these modes have not been observed for the  $^{12}\text{CO}$  and  $^{13}\text{CO}$

(25) (a) Collman, J. P.; Brauman, J. I.; Halbert, T. R.; Suslick, K. S. *Proc. Natl. Acad. Sci. U.S.A.* **1976**, *73*, 3333–3337. (b) Collman, J. P.; Brauman, J. I.; Collins, T. J.; Iverson, B. L.; Lang, G.; Pettman, R. B.; Sessler, J. L.; Walters, M. A. *J. Am. Chem. Soc.* **1983**, *105*, 3038–3052.  
(26) (a) Ricard, L.; Weiss, R.; Momenteau, M. *J. Chem. Soc., Chem. Commun.* **1986**, 818–820. (b) Fisher, J.; Weiss, R.; Momenteau, M. Unpublished results.

(27) (a) Li, X.-Y.; Spiro, T. G. *J. Am. Chem. Soc.* **1988**, *110*, 6024–6033. (b) Lechner, F. *Monatsh. Chem.* **1932**, *61*, 385–396. (c) Wilson, E. B., Jr. *J. Chem. Phys.* **1939**, *7*, 1047–1052.

**Table I.**  $\nu(\text{Fe-CO})$  and  $\nu(\text{CO})$  Stretching Frequencies ( $\text{cm}^{-1}$ ) of CO Adducts of Various Fe(II) Tetraphenylporphyrin Derivatives in Benzene or Toluene Solution

| CO deriv   | $\nu(\text{Fe-}^{12}\text{CO})^a$ | $\nu(\text{Fe-}^{13}\text{CO})^a$ | $\nu(^{12}\text{CO})^b$ | $\nu(^{13}\text{CO})^b$ | ref           |
|--|-----------------------------------|-----------------------------------|-------------------------|-------------------------|---------------|
| Fe(II) "Bis(picket)(handle)porphyrins"                                   |                                   |                                   |                         |                         |               |
| $\text{Fe}^{\text{II}}[(\text{Piv})_2\text{C}_{12}](1\text{MeIm})$       | 488                               | 484                               | 1958                    | 1912                    | this work, 10 |
| $\text{Fe}^{\text{II}}[(\text{Piv})_2\text{C}_{10}](1\text{MeIm})$       | 497                               | 494                               | 1952                    | 1910                    | this work, 10 |
| $\text{Fe}^{\text{II}}[(\text{Piv})_2\text{C}_9](1\text{MeIm})$          | 506                               | 501                               | 1948                    | 1904                    | this work, 10 |
| $\text{Fe}^{\text{II}}[(\text{Piv})_2\text{C}_8](1\text{MeIm})$          | 515                               | 510                               | 1948                    | 1904                    | this work, 10 |
|  | 497                               | 493                               |                         |                         |               |
| Fe(II) "Picket Fence"  |                                   |                                   |                         |                         |               |
| $\text{Fe}^{\text{II}}[(\text{Piv})_4](1\text{MeIm})$                    | 489                               | 485                               | 1969                    | ND <sup>c</sup>         | 24c, 25a      |
| Fe(II) Tetraphenylporphyrin  |                                   |                                   |                         |                         |               |
| $\text{Fe}^{\text{II}}[\text{TPP}](1\text{MeIm})$                        | 486                               | ND                                | 1969.5                  | ND                      | 24c           |
| Fe(II) "Basket-Handle" Porphyrins  |                                   |                                   |                         |                         |               |
| $\text{Fe}^{\text{II}}[\text{a}(\text{C}_{12})_2](1\text{MeIm})$         | 489                               | 484                               | 1970                    | 1923                    | 10, 19b       |
| $\text{Fe}^{\text{II}}[\text{a}(\text{C}_{12})(\text{C}_{11}\text{Im})]$ | 485                               | 479                               | 1971                    | 1925                    | 19b           |
| $\text{Fe}^{\text{II}}[\text{e}(\text{C}_{12})(\text{C}_{11}\text{Im})]$ | 487                               | 482                               | 1975                    | ND                      | 19b           |
| Fe(II) "Pocket" Porphyrins   |                                   |                                   |                         |                         |               |
| $\text{Fe}^{\text{II}}[\text{PivPoc}](1\text{MeIm})$                     | ND                                | ND                                | 1964                    | ND                      | 25b           |
| $\text{Fe}^{\text{II}}[\text{TalPoc}](1\text{MeIm})$                     | ND                                | ND                                | 1963                    | ND                      | 25b           |
| $\text{Fe}^{\text{II}}[\text{MedPoc}](1\text{MeIm})$                     | ND                                | ND                                | 1954                    | 1909                    | 25b           |

<sup>a</sup>RR data. <sup>b</sup>IR data. <sup>c</sup>ND = not determined.

complexes of  $\text{Fe}^{\text{II}}[(\text{Piv})_2\text{C}_{12}](1\text{MeIm})$ , these calculated frequencies are however very close to those of all imidazole-heme-CO adducts studied so far (574–587 and 563–567  $\text{cm}^{-1}$ , respectively).<sup>27a</sup>

Figure 7A represents the frequencies calculated for the  $\nu(\text{Fe-C})$ ,  $\nu(\text{C=O})$ , and  $\delta(\text{FeCO})$  modes as a function of the bending angle ( $\theta$ ), with the  $K_1$ ,  $K_2$ , and  $H$  values kept constant. This simulation shows that decreasing the angle  $\theta$  induces a decrease of both the Fe-C and C=O stretching frequencies. On the other hand, for moderate bendings ( $180^\circ < \theta < 160^\circ$ ), the isotopic shifts induced by  $^{12}\text{CO} \rightarrow ^{13}\text{CO}$  substitution on the  $\nu(\text{Fe-C})$  and  $\nu(\text{CO})$  modes are nearly constant, being 5 and 47  $\text{cm}^{-1}$ , respectively (Figure 7B). Therefore, this calculation clearly indicates that the observed increase in frequency of the  $\nu(\text{Fe-CO})$  mode and decrease in frequency of the  $\nu(\text{CO})$  mode cannot be ascribed to any significant bending of the FeCO grouping when the handle is shortened.

These results confirm recent structural data on crystalline  $\text{Fe}^{\text{II}}[(\text{Piv})_2\text{C}_8](1\text{MeIm})(\text{CO})$  in which the Fe-CO grouping is practically linear ( $\theta = 178.3^\circ$ ) and normal to the mean heme plane.<sup>26b</sup> We may therefore assume that the CO molecule also binds the iron atom of derivatives with intermediate handle lengths ( $\text{C}_9$  and  $\text{C}_{10}$ ) in a linear and perpendicular fashion. However, the X-ray and RR data concerning  $\text{Fe}^{\text{II}}[(\text{Piv})_2\text{C}_8](1\text{MeIm})(\text{CO})$  apparently are somewhat conflicting since the former data revealed only one Fe-CO structure while the RR data indicate two conformations for this grouping. On the basis of their isotopic sensitivities and of their gradual frequency increases upon handle shortening, the  $\nu(\text{Fe-CO})$  modes at 488  $\text{cm}^{-1}$  ( $n = 12$ ), 497  $\text{cm}^{-1}$  ( $n = 10$ ), 506  $\text{cm}^{-1}$  ( $n = 9$ ), and 515  $\text{cm}^{-1}$  ( $n = 8$ ) are attributed to the linear and perpendicular Fe-CO structure observed (or expected) in the crystal structures.<sup>26</sup> On the other hand, considering its small sensitivity to  $^{12}\text{CO} \rightarrow ^{13}\text{CO}$  substitution, the 497- $\text{cm}^{-1}$  band of  $\text{Fe}^{\text{II}}[(\text{Piv})_2\text{C}_8](1\text{MeIm})(\text{CO})$  may correspond to the stretching mode of a linear, or slightly bent, FeCO grouping (Figure 7B, Table I). Since the Raman activity of a FeCO bending mode is dependent on the symmetry of the axial ligands with the porphyrin plane,<sup>24d</sup> we may therefore associate the 497- $\text{cm}^{-1}$  band with the 576- $\text{cm}^{-1}$  band ( $\delta(\text{FeCO})$ ) and assign the former band to a Fe-CO stretching mode of a tilted linear or a bent FeCO grouping. The observation of two FeCO conformers in  $\text{Fe}^{\text{II}}[(\text{Piv})_2\text{C}_8](1\text{MeIm})(\text{CO})$ , as a result of steric hindrance from the strap on the FeCO groups, should not be unique since multiple FeCO structures have been revealed for CO-myoglobin and model compounds.<sup>5,24a,d,28</sup> Along these lines, the above-

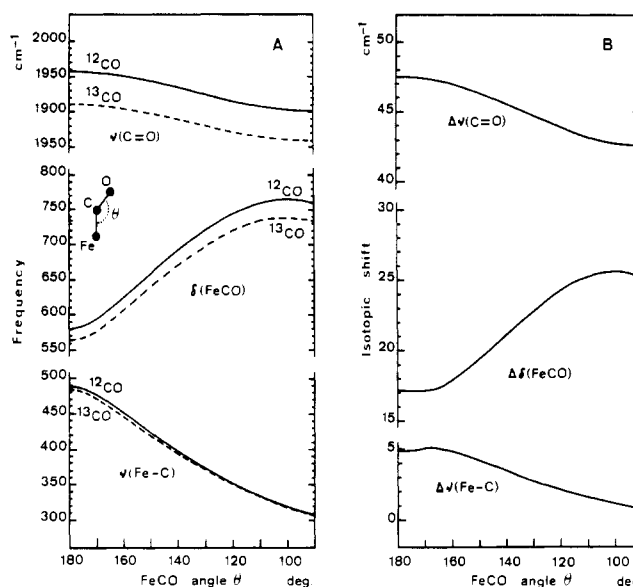


**Figure 7.** (A) Plots of the Theoretical frequencies of the  $\nu(\text{Fe-CO})$ ,  $\nu(\text{CO})$ , and  $\delta(\text{FeCO})$  modes as a function of the bending angle ( $\theta$ ) of the FeCO grouping: (solid curves)  $\nu(\text{Fe-}^{12}\text{CO})$ ,  $\nu(^{12}\text{CO})$ , and  $\delta(\text{Fe}^{12}\text{CO})$ ; (dotted curves)  $\nu(\text{Fe-}^{13}\text{CO})$ ,  $\nu(^{13}\text{CO})$ , and  $\delta(\text{Fe}^{13}\text{CO})$ . The curves are calculated by using  $K(\text{Fe-C})$ ,  $K(\text{C=O})$ , and  $H(\text{FeCO})$  values of 2.80, 14.5, and 0.22  $\text{mdyn \AA}^{-1}$ , respectively (see text). (B) Plot of the theoretical frequency shifts of the  $\nu(\text{Fe-CO})$ ,  $\nu(\text{CO})$ , and  $\delta(\text{FeCO})$  modes upon  $^{12}\text{CO} \rightarrow ^{13}\text{CO}$  isotope substitution ( $\Delta\nu(\text{Fe-CO})$ ,  $\Delta\nu(\text{CO})$ , and  $\Delta\delta(\text{FeCO})$ ) as a function of the FeCO angle ( $\theta$ ) (see text).

mentioned discrepancies between the RR data on  $\text{Fe}^{\text{II}}[(\text{Piv})_2\text{C}_8](1\text{MeIm})(\text{CO})$  in solution and X-ray data on the crystalline complex may be explained by assuming that the molecular packing forces in the crystal should favor the linear and perpendicular FeCO conformer over a linear tilted or a bent one.

Inspection of the RR and IR data displayed in Table I for CO adducts of various  $\text{Fe}^{\text{II}}\text{TPP}$  derivatives permits us to distinguish two classes among these derivatives, on the basis of their  $\nu(\text{CO})$  modes. The first class of porphyrins is characterized by a  $\nu(\text{CO})$  frequency at  $\sim 1970 \text{ cm}^{-1}$  and corresponds to porphyrins for which the solvent has access to and can interact with the bound carbonyl group. On the other hand, superprotected porphyrins ("hybrid" porphyrins and "pocket" porphyrins) exhibit  $\nu(\text{CO})$  modes at 1954–1964  $\text{cm}^{-1}$  and constitute the second class. This difference between the two classes is attributed to a "cage" effect, which in porphyrins of the second class prevents the external solvation of

(28) Makinen, M. W.; Houtchens, R. A.; Caughey, W. S. *Proc. Natl. Acad. Sci. U.S.A.* **1979**, *76*, 6042–6046.

**Table II.** Frequencies ( $\text{cm}^{-1}$ ) and Assignments of RR Bands in the 100–800- $\text{cm}^{-1}$  Region for CO and O<sub>2</sub> Complexes of Fe<sup>II</sup>[(Piv)<sub>2</sub>C<sub>n</sub>](1MeIm) in Toluene or Benzene Solutions

| Fe <sup>II</sup> [(Piv) <sub>2</sub> C <sub>12</sub> ]-<br>(1MeIm) |                | Fe <sup>II</sup> [(Piv) <sub>2</sub> C <sub>10</sub> ]-<br>(1MeIm) |                | Fe <sup>II</sup> [(Piv) <sub>2</sub> C <sub>9</sub> ]-<br>(1MeIm) |                | Fe <sup>II</sup> [(Piv) <sub>2</sub> C <sub>8</sub> ]-<br>(1MeIm) |                | assign <sup>a</sup>  |
|--|----------------|--|----------------|---|----------------|---|----------------|--|
| CO   | O <sub>2</sub> | CO   | O <sub>2</sub> | CO  | O <sub>2</sub> | CO  | O <sub>2</sub> |  |
| 787  | 786            | 786 (w)  | 787            | 787   | 787            | 787 (w)   | 786 (w)        |  |
| 748  | 745            | 746  | 747            | 744   | 746            | 746   | 747            |  |
| 731  | 728            | 735  |                | 731   | 731            | 731   | 721            |  |
| 671  | 668            | 670  | 672            | 668   | 670            | 668   | 671            |  |
| 638  | 638            | 638  | 638            | 638   | 638            | 638   | 638            | Ph mode + $\delta$ (porph)                                 |
| 575  | 577            | 574  |                | 578   | 576            | 578   | 577            |  |
|  | 563            |  | 563            |   | 560            | 576   | 563            | $\delta$ (Fe—CO)<br>$\nu$ (Fe—O <sub>2</sub> )             |
| 538  |                | 558 (w)  |                | 558   |                | 557   |                |  |
| 488  |                | 538  |                | 538   |                | 538   |                |  |
|  |                | 497  |                | 506   |                | 515   |                | $\nu$ (Fe—CO)  |
|  |                |  |                |   | 510            |   |                |  |
|  |                |  |                |   |                | 502   |                |  |
|  |                |  |                |   |                | 497   |                | $\nu$ (Fe—CO)  |
|  | 466            |  | 469            | 474   | 463            | 487 (w)   |                |  |
|  |                |  |                |   |                | 471 (w)   | 470            | $\gamma$ (pyrr)  |
|  |                |  |                |   |                | 459 (w)   |                |  |
| 440  | 447            | 442  | 448            | 443   | 444 (w)        |   | 444            | $\gamma$ (pyrr)  |
|  |                |  |                | 430 (w)   | 432 (w)        |   | 431            |  |
|  |                | 400  | 394            | 401   | 397            |   | 404            |  |
| 382  | 383            | 384  | 385            | 384   | 386            |   | 388            | $\gamma$ (porph) ( $\nu_8$ )                               |
| 320  | 322            | 321  | 327            | 320   |                |   | 320            | $\gamma$ (porph)   |
|  |                |  |                |   |                |   | 327            |  |
|  |                |  |                |   |                |   | 345            |  |
| 290  | 286            | 288 (sh)   | 288            | 283 (sh)  |                |   | 290            |  |
| 266  |                | 271  | 272            | 269   |                |   | 267            | $\gamma$ (porph)   |
| 242  | 250            | 246  | 250            |   |                |   | 255            | $\delta$ (porph)   |
| 216 (w)  | 215 (w)        |  |                | 216   | 216            | 207   |                |  |
| 189 (sh)   |                | 199  |                |   |                |   | 198 (w)        |  |
| 178  | 178            | 173  | 172            | 167   |                |   |                | $\gamma$ (C <sub>m</sub> -Ph) + $\nu$ (C <sub>m</sub> -Ph) |
| 160 (sh)   | 157            |  |                | 152   | 154 (w)        |   |                |  |
| 140 (w)  |                |  |                |   |                |   |                |  |

<sup>a</sup> See text and ref 14 and 16 for assignments; w = weak band; sh = shoulder.

bound CO. Furthermore, the decrease of the  $\nu$ (CO) stretching frequency from 1958 to 1948  $\text{cm}^{-1}$  as one goes from Fe<sup>II</sup>[(Piv)<sub>2</sub>C<sub>12</sub>](1MeIm)(CO) to Fe<sup>II</sup>[(Piv)<sub>2</sub>C<sub>8</sub>](1MeIm)(CO) may be explained by changes in local polarity.<sup>29</sup> A local ligand solvation may result from interactions of the CO bound to the iron atom with the secondary amide groups present in the chain and two pickets, X-ray data indeed have shown that, in the C<sub>12</sub> derivative, the four  $\delta^-\text{O}=\text{C}-\text{N}-\text{H}^{\delta+}$  dipoles point toward the metal atom.<sup>26a</sup> On the other hand, the crystal structure of the C<sub>8</sub> derivative clearly indicates a rotation of one of the two amide groups of the chain by about 90°.<sup>26b</sup> In this derivative, the chain tension induces the corresponding amide dipole to orient out of the coordination sphere of the iron atom, thus likely resulting in a decrease of the local solvation of the bound CO.

On the other hand, the Fe—CO bond appears weakly sensitive to CO solvation, as the  $\nu$ (Fe—CO) mode is observed in the 486–489- $\text{cm}^{-1}$  range for Fe<sup>II</sup>TPP(1MeIm)(CO), Fe<sup>II</sup>[(Piv)<sub>4</sub>](1MeIm)(CO), and Fe<sup>II</sup>[(Piv)<sub>2</sub>C<sub>12</sub>](1MeIm)(CO).

Taking the Fe—CO and C—O distances in Fe<sup>II</sup>[(Piv)<sub>2</sub>C<sub>12</sub>](1MeIm)(CO) as equal to 1.728 and 1.149 Å,<sup>26a</sup> we can calculate the corresponding bond lengths of the other three Fe<sup>II</sup>[(Piv)<sub>2</sub>C<sub>n</sub>](1MeIm)(CO) complexes by using a modified Badger rule<sup>30</sup> and  $d_{ij}$  values of 0.75 and 0.68 Å for the Fe—C and C—O bonds, respectively.<sup>12b,30b</sup> This calculation gives Fe—CO bond lengths of 1.716, 1.705, and 1.694 Å and C—O bond distances of

1.150, 1.151, and 1.151 Å. C—O bond distances clearly are less affected than the Fe—C bond lengths by handle shortening.

Yu et al.<sup>24</sup> recently studied the steric hindrance effect exerted on the FeCO grouping by a hydrocarbon chain on carbonyl-“strapped” ferrohemes. As in the picket-handle porphyrin series, increases in  $\nu$ (Fe—CO) stretching frequencies and decreases in  $\nu$ (CO) stretching frequencies were observed with decreasing chain length. However, an FeCO bending vibration was detected at 574–579  $\text{cm}^{-1}$ . These results were interpreted as an increased tilt of a nearly linear Fe—C—O moiety.<sup>24d</sup> Different conformations of the Fe—CO grouping in the two series of compounds may be explained by the differences in chemical nature of both the protecting strap and the porphyrin substituents at the meso positions. The chemical nature of the strap is expected to influence the shape and the size of the CO pocket while that of the latter effect promotes different  $\pi$ -electronic structures in the two porphyrin systems. Furthermore, with use of Dreiding molecular models, the distance between the top of the strap and the iron atom is smaller in Yu's models than in the Fe<sup>II</sup>[(Piv)<sub>2</sub>C<sub>n</sub>] derivatives. Therefore, the steric central effects are more sizable in the former derivatives.

In addition to those observed in the Fe—CO stretching frequencies, RR spectra of the Fe<sup>II</sup>[(Piv)<sub>2</sub>C<sub>n</sub>](1MeIm)(CO) derivatives exhibit several other differences in frequencies and in relative intensities of low-frequency porphyrin bands (Table II, 400–600- $\text{cm}^{-1}$  regions shown in Figure 6). These spectral variations result from different porphyrin structures induced by bonding and nonbonding interactions between the ligands, porphyrin, and handle.

Figure 4 shows that mode  $\nu_2$  of Fe<sup>II</sup>[(Piv)<sub>2</sub>C<sub>12</sub>](1MeIm)(CO) occurs at 1561  $\text{cm}^{-1}$ . If the  $K$  and  $A$  values are taken as 248.4  $\text{cm}^{-1} \text{Å}^{-1}$  and 8.29 Å, respectively (line I in Figure 5), a porphyrin core size of 2.006 Å is calculated by using eq 1. The crystal structure has shown that this diameter is actually very close to this value, being  $1.999 \pm 0.003 \text{ Å}$ .<sup>26a</sup> Mode  $\nu_2$  occurs at 1560, 1559, and 1557  $\text{cm}^{-1}$  for Fe<sup>II</sup>[(Piv)<sub>2</sub>C<sub>n</sub>](1MeIm)(CO) ( $n = 10,$

(29) (a) Lavalette, D.; Tetreau, C.; Mispelter, J.; Momenteau, M.; Lhoste, J. M. *Eur. J. Biochem.* **1984**, *145*, 555–565. (b) Traylor, T. G.; Koga, N.; Deardurff, L. A. *J. Am. Chem. Soc.* **1985**, *107*, 6504–6510. (c) Lexa, D.; Momenteau, M.; Savéant, J. M.; Xu, F. *Inorg. Chem.* **1986**, *25*, 4857–4865.

(30) (a) The Fe—CO and C—O bond length variations in Fe<sup>II</sup>[(Piv)<sub>2</sub>C<sub>n</sub>](1MeIm)(CO) may be estimated from the stretching frequencies ( $\nu$  and  $\nu'$ ) by using the following modified Badger rule:<sup>28b</sup>  $(\nu/\nu')^2 = [(r_e' - d_{ij})/(r_e - d_{ij})]^3$ , where  $r_e$  and  $r_e'$  are the equilibrium bond distances (Å),  $d_{ij}$  being a constant depending on the atoms involved in the bond. (b) Herschbach, D. R.; Laurie, V. W. *J. Chem. Phys.* **1961**, *35*, 458–463.

**Table III.** Frequencies ( $\text{cm}^{-1}$ ) and Assignments of RR Bands in the 800–1650- $\text{cm}^{-1}$  Region for CO and  $\text{O}_2$  Complexes of  $\text{Fe}^{\text{II}}[(\text{Piv})_2\text{C}_n](1\text{MeIm})$  in Toluene or Benzene Solutions

| $\text{Fe}^{\text{II}}[(\text{Piv})_2\text{C}_{12}]-(1\text{MeIm})$ |              | $\text{Fe}^{\text{II}}[(\text{Piv})_2\text{C}_{10}]-(1\text{MeIm})$ |              | $\text{Fe}^{\text{II}}[(\text{Piv})_2\text{C}_9]-(1\text{MeIm})$ |              | $\text{Fe}^{\text{II}}[(\text{Piv})_2\text{C}_8]-(1\text{MeIm})$ |              | assign <sup>a</sup>                         |
|---|--------------|---|--------------|--|--------------|--|--------------|---|
| CO  | $\text{O}_2$ | CO  | $\text{O}_2$ | CO   | $\text{O}_2$ | CO   | $\text{O}_2$ |   |
| 1605  | 1605         | 1605  | 1605         | 1607   | 1607         | 1606   | 1606         | Ph mode                                     |
| 1587  | 1587         | 1589  | 1587         | 1589   | 1589         | 1590   | 1586         | Ph mode                                     |
|   | 1582         |   |              |  |              |  |              |   |
| 1561  | 1563         | 1560  | 1562         | 1559   | 1562         | 1557   | 1560         | $\nu(\text{C}_b-\text{C}_b)$ ( $\nu_2$ )    |
| 1534  | 1535         |   | 1533         |  |              |  | 1526         |   |
| 1502  | 1503         | 1499  | 1501         | 1495   | 1498         | 1493   | 1494         | $\nu(\text{C}_b-\text{C}_b)$ ( $\nu_{12}$ ) |
|   |              |   |              | 1482   | 1490         |  |              |   |
| 1470  | 1470         | 1474  | 1472         | 1467   | 1457         | 1452   | 1465         | $\nu(\text{C}_a-\text{C}_b)$ ( $\nu_3$ )    |
| 1440  | 1442         | 1441  | 1440         | 1445   | 1438         |  | 1442         |   |
|   |              | 1384  |              | 1382   |              | 1386   |              | $\nu(\text{C}_a-\text{N})$ ( $\nu_{13}$ )   |
| 1363  | 1367         | 1363  | 1368         | 1365   | 1369         | 1365   | 1370         | $\nu(\text{C}_a-\text{N})$ ( $\nu_4$ )      |
| 1333  | 1333         |   |              |  |              |  | 1333         |   |
| 1307  | 1306         |   | 1311         |  | 1313         |  | 1312         |   |
|   |              | 1302  |              |  |              |  |              |   |
| 1280  | 1280         | 1282  | 1282         | 1282   | 1285         | 1282   | 1282         |   |
| 1252  | 1252         | 1252  | 1254         | 1255   | 1256         | 1255   | 1255         | Ph mode                                     |
| 1205  | 1205         | 1207  | 1208         | 1208   | 1209         | 1208   | 1209         |   |
|   | 1160         |   | 1160         | 1157 (w)   | 1161         |  | 1160         |   |
|   |              |   |              |  |              | 1151   | 1152         |   |
| 1107  | 1107         | 1107  | 1107         | 1107   | 1109         | 1106   | 1106         |   |
| 1077  | 1076         | 1077  | 1078         | 1078   | 1080         | 1077   | 1078         | $\delta(\text{C}_b-\text{H})$ ( $\nu_5$ )   |
| 1043  | 1043         | 1045  | 1043         | 1045   | 1043         | 1045   | 1044         | Ph mode                                     |
|   |              |   |              |  |              |  | 1004         | $\nu(\text{C}_a-\text{C}_m)$ ( $\nu_6$ )    |
|   |              |   |              |  |              | 908  | 916          |   |
| 890   | 890          | 892   |              | 892  | 895          | 894  | 895          | $\delta(\text{porph})$ ( $\nu_7$ )          |
|   |              |   | 844          |  | 846          |  |              |   |
| 821   | 820          |   | 827          | 823  | 830          | 831  | 830          |   |
| 797   | 799          | 808   | 802          | 800  | 802          | 807  | 802          |   |

<sup>a</sup> See text and ref 14 and 16 for assignments; w = weak band.

9, 8), respectively (Figure 4, Table III). These values correspond to calculated Ct–N distances of 2.010, 2.014, and 2.022 Å, respectively. Since the handle shortening from  $\text{C}_{12}$  to  $\text{C}_8$  is not expected to favor a core expansion, we suggest that the decrease in frequency of  $\nu_2$  reflects more an increased porphyrin deformation (ruffling and/or doming)<sup>20b</sup> than a change in the core size. This conclusion is in agreement with the recent X-ray data on the  $\text{C}_8$  derivative, which indicate a Ct–N distance of 1.981 Å.<sup>26b</sup>

The  $\nu_4$  mode of  $\text{Fe}^{\text{II}}[(\text{Piv})_2\text{C}_n](1\text{MeIm})(\text{CO})$  exhibits a slight increase of frequency from 1363 to 1365  $\text{cm}^{-1}$  as the handle length is decreased (Figure 3, Table III). It is well-known that this C–N(pyrrole) breathing mode is sensitive to the competition between the axial ligands and the porphyrin ring for back-bonding of the  $d_\pi$  electrons.<sup>12</sup> The observed increase of  $\nu_4$  frequency may therefore be tentatively explained on the basis of a slight increased  $\pi$  electron density at the Fe–CO bond (however, see last sentence of the Dioxygen Adducts section).

**Dioxygen Adducts.** Brunner<sup>31</sup> has assigned a  $^{18}\text{O}_2$ -sensitive RR band at 570  $\text{cm}^{-1}$  to the Fe– $\text{O}_2$  stretching mode of oxyhemoglobin. Benko and Yu<sup>32</sup> have since questioned this assignment and have suggested that this band should rather correspond to a Fe– $\text{O}_2$  bending mode. However, by combining isotopic studies with normal-coordinate treatments, Bajdor et al.<sup>33</sup> recently showed that the 570- $\text{cm}^{-1}$  band is a mode essentially involving the Fe– $\text{O}_2$  stretch, the deformation mode being expected in the 250–280- $\text{cm}^{-1}$  region.

Figure 8 displays the 500–650- $\text{cm}^{-1}$  region of RR spectra of oxygenated complexes of  $\text{Fe}^{\text{II}}[(\text{Piv})_2\text{C}_n](1\text{MeIm})$  in benzene or toluene solution. Specific bands observed at 560–563  $\text{cm}^{-1}$  in these spectra are downshifted by 23–24  $\text{cm}^{-1}$  upon  $^{16}\text{O}_2 \rightarrow ^{18}\text{O}_2$  isotope exchange (Figure 8). These shifts are close to those induced by the same substitution in oxyhemoproteins and oxygenated model compounds (20–24  $\text{cm}^{-1}$ ).<sup>14b,24b,34</sup> The 560–563- $\text{cm}^{-1}$  bands of

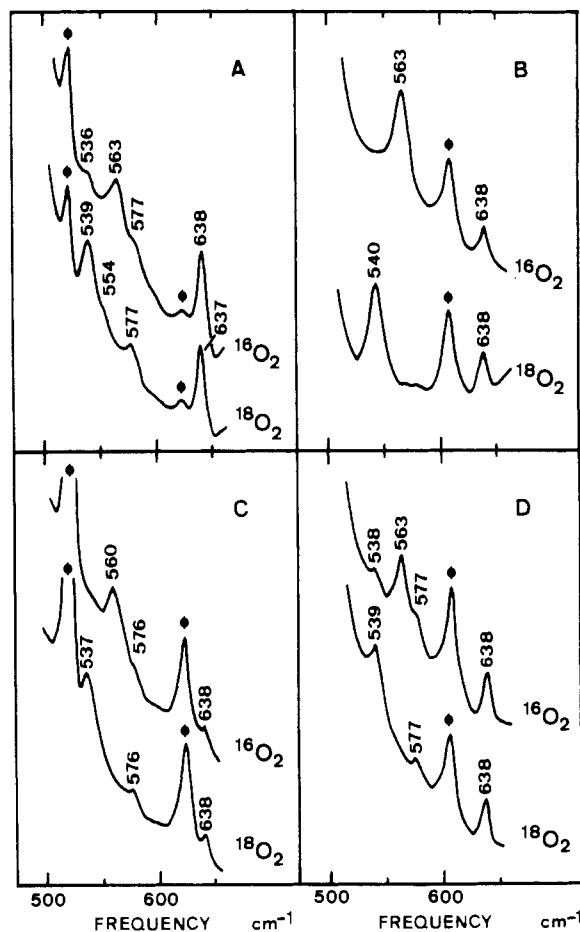


**Figure 8.** Oxygen isotope effect on the low-frequency regions (500–650  $\text{cm}^{-1}$ ) of resonance Raman spectra of  $\text{Fe}^{\text{II}}[(\text{Piv})_2\text{C}_n](1\text{MeIm})(\text{O}_2)$  in toluene or benzene solutions (summation of four scans;  $\phi$  designs solvent bands): (A)  $n = 12$ ; (B)  $n = 10$ ; (C)  $n = 9$ ; (D)  $n = 8$ .

(31) Brunner, H. *Naturwissenschaften* **1974**, *61*, 129–130.

(32) Benko, B.; Yu, N.-T. *Proc. Natl. Acad. Sci. U.S.A.* **1983**, *80*, 7042–7046.

(33) Bajdor, K.; Oshio, H.; Nakamoto, K. *J. Am. Chem. Soc.* **1984**, *106*, 7273–7274.



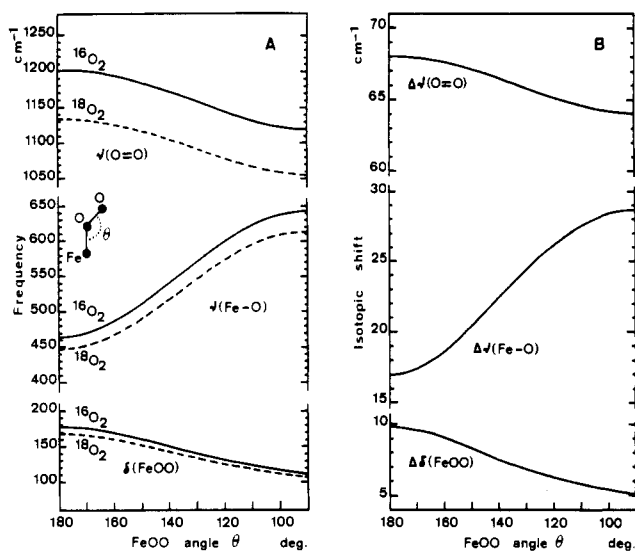


**Figure 9.** Plots of the theoretical  $\nu(\text{Fe}-\text{O}_2)$ ,  $\nu(\text{O}_2)$ , and  $\delta(\text{FeO}_2)$  frequencies (A) and of the theoretical frequency shifts ( $\Delta\nu(\text{Fe}-\text{O}_2)$ ,  $\Delta\nu(\text{O}_2)$ , and  $\Delta\delta(\text{FeO}_2)$ ) upon  $^{16}\text{O}_2 \rightarrow ^{18}\text{O}_2$  isotope substitution (B) as a function of the Fe-O-O angle ( $\theta$ ). The curves are calculated by using  $K(\text{Fe}-\text{O})$ ,  $K(\text{O}=\text{O})$ , and  $H(\text{FeOO})$  values of 2.98, 5.90, and 0.025  $\text{mdyn } \text{\AA}^{-1}$ , respectively (see text).

$\text{Fe}^{\text{II}}[(\text{Piv})_2\text{C}_n](1\text{MeIm})(\text{O}_2)$  complexes are therefore assigned to the  $\nu(\text{Fe}-\text{O}_2)$  stretching mode. We note that these frequencies are low compared to those of  $\text{Fe}^{\text{II}}[(\text{Piv})_4](1\text{MeIm})(\text{O}_2)$  (568–571  $\text{cm}^{-1}$ ) and of oxyhemoproteins (567–573  $\text{cm}^{-1}$ ).<sup>14b,17a,24c,g,31,34</sup> The possible origin for these low values is discussed in the following.

The Fe-O<sub>2</sub> stretch is expected to be dependent upon bond strength, Fe-O-O geometry, and H-bonding at the terminal oxygen. Occurrence of H-bonding between bound O<sub>2</sub> and one amide proton of the porphyrin handle has been demonstrated by IR spectroscopy and NMR.<sup>10,35</sup> On the other hand, the amide N-H groups of "pickets" are unable to contract H-bonding with the ligand in the two pickets and the handle,<sup>10,35</sup> as well as in the four picket derivatives.<sup>6a,c</sup>

Hydrogen bond formation is expected to favor  $\text{Fe}^{\delta+}-\text{O}_2^{\delta-}$  polarization and, therefore, to induce a frequency decrease of the  $\nu(\text{O}_2)$  mode and a frequency increase of the  $\nu(\text{Fe}-\text{O}_2)$  mode.<sup>36</sup> The lower frequency of the  $\nu(\text{Fe}-\text{O}_2)$  mode of  $\text{Fe}^{\text{II}}[(\text{Piv})_2\text{C}_n](1\text{MeIm})(\text{O}_2)$  relative to that of  $\text{Fe}^{\text{II}}[(\text{Piv})_4](1\text{MeIm})(\text{O}_2)$  thus cannot be explained by the N-H...O<sub>2</sub> hydrogen bond formation observed for the former derivative. However, this H-bonding can control the orientation and the conformation of the Fe-O<sub>2</sub> grouping. With the phenyl groups orthogonal to the mean heme plane, an unconstrained ligand orientation with the Fe-O-O plane nearly bisecting the N(pyrrole)-Fe-N(pyrrole) heme axis is dictated by this H-bonding (Figure 1). As mentioned earlier for the Fe-CO bond, the conformation of the Fe-O-O group may be affected by a tilting of the Fe-O<sub>2</sub> bond relative to the heme normal and/or by a change in the Fe-O-O angle. A bond tilting is expected to increase the  $\nu(\text{Fe}-\text{O}_2)$  stretching mode in a way similar to that observed for the  $\nu(\text{Co}-\text{O}_2)$  stretching mode of cobalt oxyhemoglobin from *Chironomus thummi thummi*.<sup>37</sup> In order to estimate the influence of a Fe-O-O bond angle variation on the Fe-O<sub>2</sub> stretching frequency, we have performed a normal-coordinate calculation on a simple triatomic Fe-O-O model. For this purpose, the crystallographic ( $d(\text{Fe}-\text{O}) = 1.75 \text{ \AA}$ ;  $d(\text{O}=\text{O})$

$= 1.16 \text{ \AA}$ ;  $\angle\text{Fe}-\text{O}-\text{O} = 131^\circ$ ) and vibrational data ( $\nu(\text{Fe}-\text{O}_2) = 568 \text{ cm}^{-1}$ ;  $\nu(\text{O}_2) = 1159 \text{ cm}^{-1}$ ) obtained for  $\text{Fe}^{\text{II}}[(\text{Piv})_4](1\text{MeIm})(\text{O}_2)$ <sup>6c,14b,25a</sup> have been used. Force constants of 2.98, 5.90, and 0.025  $\text{mdyn } \text{\AA}^{-1}$  are so calculated for  $K_1(\text{Fe}-\text{O})$ ,  $K_2(\text{O}=\text{O})$ , and  $H(\text{FeOO})$ , respectively. Assuming that these force constants remain constant with the Fe-O-O angle  $\theta$ , the theoretical frequency dependences shown in Figure 9A are obtained for the  $\nu(\text{Fe}-^{16}\text{O}_2)$ ,  $\nu(\text{Fe}-^{18}\text{O}_2)$ ,  $\nu(^{16}\text{O}_2)$ ,  $\nu(^{18}\text{O}_2)$ ,  $\delta(\text{Fe}-^{16}\text{O}_2)$ , and  $\delta(\text{Fe}-^{18}\text{O}_2)$  modes as a function of  $\theta$ . Figure 9B represents the calculated frequency shifts of these modes upon oxygen isotope substitution, as a function of angle  $\theta$ . These figures clearly show that a slight increase of the  $\theta$  value from 131 to 135° induces a large downshift of the  $\nu(\text{Fe}-\text{O}_2)$  stretching mode from 568 to 556  $\text{cm}^{-1}$ , the oxygen isotope shift remaining in the 23–24- $\text{cm}^{-1}$  range. Therefore, the most plausible explanation for the comparatively low frequencies of the  $\nu(\text{Fe}-\text{O}_2)$  mode in  $\text{Fe}^{\text{II}}[(\text{Piv})_2\text{C}_n](1\text{MeIm})(\text{O}_2)$  derivatives is that a frequency decrease of this mode, due to a Fe-O-O bond angle slightly larger than the "four pickets" derivatives, overcompensates the frequency increase expected from H-bonding of the oxygen ligand in the two-picket-one-handle derivatives.

In the higher frequency regions of RR spectra modes,  $\nu_2$  and  $\nu_4$  are upshifted by 2–3 and 4–5  $\text{cm}^{-1}$ , respectively, on going from CO to O<sub>2</sub> complexes of  $\text{Fe}^{\text{II}}[(\text{Piv})_2\text{C}_n](1\text{MeIm})$  (Figures 3 and 4; Table III). This effect is due to a stronger  $\pi$ -acidity of O<sub>2</sub> than that of CO.<sup>12</sup> The effects of "handle" shortening on the  $\nu_2$  and  $\nu_4$  modes of the oxygenated complexes are the same as for the carbonylated complexes, i.e. a decrease of the  $\nu_2$  frequency and an increase of the  $\nu_4$  frequency (Table III). The decrease of the  $\nu_2$  frequency is therefore also interpreted as corresponding to increasing deformations of the porphyrin macrocycle rather than to a core expansion (cf. previous section).

In the preceding section, the frequency increase of mode  $\nu_4$  of carbonylated complexes of  $\text{Fe}^{\text{II}}[(\text{Piv})_2\text{C}_n](1\text{MeIm})$  upon handle shortening was interpreted as resulting from increased strength of the Fe-CO bond. However, for the oxygenated complexes, whereas the  $\nu_4$  frequency increases, the  $\nu(\text{Fe}-\text{O}_2)$  stretching mode is nearly unaffected. Therefore, the  $\nu_4$  frequency increase is attributed to an increase of macrocycle deformations upon handle shortening of O<sub>2</sub> complexes of  $\text{Fe}^{\text{II}}[(\text{Piv})_2\text{C}_n](1\text{MeIm})$ . Furthermore, considering the similar amplitude of frequency shifts of the  $\nu_4$  modes of O<sub>2</sub> and CO derivatives of  $\text{Fe}^{\text{II}}[(\text{Piv})_2\text{C}_n](1\text{MeIm})$  (Table II), the downshift of this mode in the CO series should have its origin in the increased porphyrin deformation rather than in the increased Fe-CO bond strength.

**Structures of  $\text{Fe}^{\text{II}}[(\text{Piv})_2\text{C}_n]$  Derivatives in Relation to Ligand Affinity.** The present structural data can be usefully compared with the kinetic rate constants for the binding of CO and O<sub>2</sub> with  $\text{Fe}^{\text{II}}[(\text{Piv})_2\text{C}_n](1\text{MeIm})$ . It has been shown that decreasing the handle length induces a gradual decrease of the association rates of CO and O<sub>2</sub>.<sup>10</sup> RR spectra of the five-coordinated deoxygenated forms indicated that slight distortions at the porphyrin periphery, the phenyl groups, and the 1MeIm coordination occur for the C<sub>8</sub> derivative only. Moreover, as these modifications are expected to be energetically negligible, the observed decrease of the on-rate constant primarily originates in the smaller size of the ligand cavity.

On the other hand, no major change is observed in the CO dissociation rates when the "handle" length decreases. A different situation prevails for the dissociation rates of O<sub>2</sub> which are decreased by a factor of 60 from the C<sub>12</sub> to the C<sub>8</sub> derivative.<sup>10</sup>

X-ray crystal structures<sup>26</sup> and the present RR spectra show that the Fe-CO grouping is essentially linear and perpendicular to the heme plane. Furthermore, these vibrational data demonstrate that the handle shortening promotes deformation of the porphyrin macrocycle and a shortening of the Fe-CO bond. Therefore, the off-rate constants of the CO group and the strengths of the Fe-CO bond of  $\text{Fe}^{\text{II}}[(\text{Piv})_2\text{C}_n](1\text{MeIm})(\text{CO})$  complexes cannot be directly related. Evidence for an inverse correlation was previously noted between the CO binding equilibrium constant and the Fe-CO bond strength of  $\text{Fe}^{\text{II}}[(\text{Piv})_4](\text{CO})$  complexed with hindered or unhindered axial bases.<sup>24c</sup> However, in the

- (34) (a) Duff, L. L.; Appelman, E. H.; Shriver, D. F.; Klotz, I. M. *Biochem. Biophys. Res. Commun.* **1979**, *90*, 1098–1103. (b) Walters, M. A.; Spiro, T. G.; Suslick, K. S.; Collman, J. P. *J. Am. Chem. Soc.* **1980**, *102*, 6857–6858.
- (35) Mispelter, J.; Momenteau, M.; Lavalette, D.; Lhoste, J. M. *J. Am. Chem. Soc.* **1983**, *105*, 5165–5166.
- (36) Odo, J.; Imai, H.; Kyuno, E.; Nakamoto, K. *J. Am. Chem. Soc.* **1988**, *110*, 742–748.
- (37) Thompson, H. M.; Yu, N.-T.; Gersonde, K. *Biophys. J.* **1987**, *51*, 289–295.

present model compounds, the steric strain induced in the porphyrin cycle by the handle appears to be accommodated on several bonds by macrocycle deformations (ruffling and/or doming). Therefore, the near-constant values of CO dissociation rates is most probably due to these increased porphyrin distortions, which should energetically compensate the observed Fe—CO bond strengthening.

The oxygenated complexes of  $\text{Fe}^{\text{II}}[(\text{Piv})_2\text{C}_n](1\text{MeIm})$  provide a presently unique example of model compounds in which the  $\nu(\text{Fe—O}_2)$  stretching mode occurs at such a low frequency ( $560\text{--}563\text{ cm}^{-1}$ ). This effect is interpreted as reflecting antagonist effects between H-bonding at the  $\text{O}_2$  moiety and deformation of the Fe—O—O angle. The nearly constant frequency of the  $\nu(\text{Fe—O}_2)$  stretching mode shows that the decrease of  $\text{O}_2$  off-rates upon handle shortening is not directly related to the Fe— $\text{O}_2$  bond strength. On the other hand, as in the case of carbonylated complexes, handle shortening of oxygenated complexes increases porphyrin deformations, but this effect has no compensation upon the Fe— $\text{O}_2$  bond strength. Therefore, the decrease of  $\text{O}_2$  off-rates essentially originates in increased porphyrin distortions upon handle shortening.

The binding site of hemoproteins represents a way of preventing poisoning from CO produced by the cellular catabolism.<sup>2c</sup> Experimental support for this proposal has come from observations of tilted or bent Fe—CO structures in hemoproteins, as compared to the linear and perpendicular structures of model complexes.<sup>3,4</sup>

The present data however suggest another mechanism by which hemoproteins may differentiate between  $\text{O}_2$  and CO, the strong Fe—CO bond being destabilized by porphyrin deformations. Bringing some support to this proposal, the Raman-active, high-frequency modes of the  $\text{O}_2$  and CO complexes of hemoglobin, myoglobin, and leghemoglobin exhibit some frequency dispersion,<sup>3b</sup> suggesting variable deformation of the heme cycle. Unfortunately, however, Raman data are not yet available for imidazole—Fe(II)—protoporphyrin—ligand model compounds, which alone would allow such deformations to be unambiguously characterized. Yet, the present data point at the importance of the macrocycle structure and, hence, of the electron distribution over the porphyrin in this mechanism of ligand discrimination.

**Acknowledgments.** Helpful comments from Prof. T. G. Spiro about this work are gratefully acknowledged. This work was supported in part by grants from the Centre National de la Recherche Scientifique (UA 1089 and RCP No. 280) and the Institut National de la Santé et de la Recherche Médicale (U 219 and CRC No. 861012).

- (38) (a) Spiro, T. G.; Strekas, T. C. *J. Am. Chem. Soc.* **1974**, *96*, 338–345. (b) Dallinger, R. F.; Nestor, J. R.; Spiro, T. G. *J. Am. Chem. Soc.* **1978**, *100*, 6251–6252. (c) Armstrong, R. S.; Irwin, M. J.; Wright, P. E. *Biochem. Biophys. Res. Commun.* **1980**, *95*, 682–689. (d) Rousseau, D. L.; Ondrias, M. R.; LaMar, G. N.; Kong, S. B.; Smith, K. M. *J. Biol. Chem.* **1983**, *258*, 1740–1746.

Contribution from the Central Institute of Nuclear Research Rossendorf, PF 19, 8051-Dresden, GDR, Department of Chemistry, Karl-Marx-University, 7010-Leipzig, GDR, Department of Sciences, Technical University, 7010-Leipzig, GDR, and Crystallography Laboratory, University of Nijmegen, 6525 Nijmegen, The Netherlands

## Synthesis and Characterization of Technetium(V) Complexes with *N*-(Thiocarbamoyl)benzamidines. X-ray Crystal Structure of Bis[*N*-(*N,N*-diethylthiocarbamoyl)benzamidinato]oxotechnetium(V) Chloride, $[\text{TcO}(\text{Et}_2\text{tcb})_2]\text{Cl}$

U. Abram,\*† R. Muenze,† J. Hartung,‡ L. Beyer,‡ R. Kirmse,§ K. Koehler,§ J. Stach,§ H. Behm,|| and P. T. Beurskens||

Received March 31, 1988

Technetium(V) complexes of the forms  $\text{TcNL}_2$  and  $[\text{TcOL}_2]\text{Cl}$  ( $\text{L} = \text{Et}_2\text{tcb}^-$ ,  $\text{morphtcb}^-$ ,  $\text{piptcb}^-$ ) with *N*-(thiocarbamoyl)-benzamidinato ( $\text{tcb}^-$ ) ligands have been synthesized and characterized by elemental analysis and IR,  $^1\text{H}$  NMR, and UV/vis spectroscopy. Selected compounds have been studied by EI and FAB mass spectrometry, including the MIKE technique. A single-crystal X-ray structure determination shows that the cation of bis[*N*-(*N,N*-diethylthiocarbamoyl)benzamidinato]oxotechnetium(V) chloride, formula weight 618.5, has a square-pyramidal structure with cis-coordinated ligands. This complex crystallizes in the triclinic space group  $P\bar{1}$  with  $a = 10.87(2)\text{ \AA}$ ,  $b = 11.587(2)\text{ \AA}$ ,  $c = 12.374(2)\text{ \AA}$ ,  $\alpha = 91.94(2)^\circ$ ,  $\beta = 106.04(2)^\circ$ ,  $\gamma = 112.18(2)^\circ$ , and  $V = 1370.4(4)\text{ \AA}^3$  with  $Z = 2$  for 4723 independent observed reflections.

### Introduction

The widespread use of complex compounds of the metastable nuclide  $^{99\text{m}}\text{Tc}$  ( $\gamma$ -emitter with  $E = 140\text{ keV}$  and half-life  $t_{1/2} = 6\text{ h}$ ) in diagnostic nuclear medicine<sup>1–3</sup> has resulted in a growing interest in the basic coordination chemistry of technetium,<sup>4–6</sup> which differs markedly from that of rhenium. This is mainly due to the different redox behaviors of these two group 7 elements.<sup>6</sup>

The further exploration of technetium chemistry is a main factor in the development of new Tc radiopharmaceuticals. In recent years cationic and neutral Tc complexes entered the center of interest as potential tracers for myocardial and brain scintigraphy. Of particular importance are coordination compounds, the lipo-

philic and polar properties of which can easily be varied by simple substitutions in the molecular framework of the ligands to optimize the biodistribution of the potential radiopharmaceutical preparations. This has been shown for various complex types including ditertiary phosphine,<sup>7,8</sup> alkyl isocyanide,<sup>9</sup> amino oxime,<sup>10</sup> amino

- (1) Subramanian, S. G.; Rhodes, B. A.; Cooper, J. F.; Sodd, V. J. *Radiopharmaceuticals*; The Society of Nuclear Medicine: New York, 1975. (2) Srivastava, S. C.; Richards, P. *Radiotracers for Medical Applications*; CRC: Boca Raton, FL, 1983. (3) Muenze, R. *Isotopenpraxis* **1983**, *19*, 401. (4) Jones, A. G.; Davison, A. *Int. J. Appl. Radiat. Isot.* **1982**, *33*, 867. (5) Davison, A.; Jones, A. G. *Int. J. Appl. Radiat. Isot.* **1982**, *33*, 881. (6) Deutsch, E.; Libson, K.; Jurisson, S.; Lindoy, L. F. *Prog. Inorg. Chem.* **1983**, *75*. (7) Schwochau, K. *Radiochim. Acta* **1983**, *32*, 139. (8) Libson, K.; Barnett, B. L.; Deutsch, E. *Inorg. Chem.* **1983**, *22*, 1695. (9) Vanderheyden, J. L.; Ketring, A. R.; Libson, K.; Heeg, M. J.; Roecker, L.; Motz, P.; Whittle, R.; Elder, R. C.; Deutsch, E. *Inorg. Chem.* **1984**, *23*, 3184.

\* To whom correspondence should be addressed.

† Central Institute of Nuclear Research Rossendorf.

‡ Technical University.

§ Karl-Marx-University.

|| University of Nijmegen.